Development of Distillation Column Model for MLNG Depropanizer Column - Incorporating Redlich-Kwong Equation of State

By

Chai Ai Ling

Dissertation submitted in partial fulfillment of
the requirements for the
Bachelor of Engineering (Hons)
(Chemical Engineering)

January 2005

Universiti Teknologi PETRONAS
Bandar Seri Iskandar
31750 Tronoh
Perak Darul Ridzuan
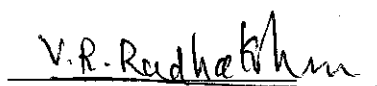
CERTIFICATION OF APPROVAL

Development of Distillation Column Model for MLNG Depropanizer Column - Incorporating Redlich-Kwong Equation of State

by

Chai Ai Ling

A project dissertation submitted to the

Chemical Engineering Programme

Universiti Teknologi PETRONAS

in partial fulfillment of the requirements for the

BACHELOR OF ENGINEERING (Hons)

(CHEMICAL ENGINEERING)

Approved by,

V. R. Radhakrishnan

(Prof. Dr. V. R. Radhakrishnan)

Main Supervisor

UNIVERSITI TEKNOLOGI PETRONAS

TRONOH, PERAK

October 2004

i

CERTIFICATION OF ORIGINALITY

This is to certify that I am responsible for the work submitted in this project, that the original work is my own except as specified in the references and acknowledgements, and that the original work contained herein have not been undertaken or done by unspecified sources or persons.

_____

CHAI AI LING

ABSTRACT

The growing importance of propane as an alternative fuel and refrigerant has intensified the need to optimize the production of propane from the MLNG depropanizer column. In order to achieve on-line optimization for the depropanizer column using Advanced Process Control Techniques (APC), an accurate distillation column model is essential. This report presents the preliminary work in developing an accurate distillation column model for the depropanizer column. The depropanizer column modeled is a 47-stage column processing feed which contains Propane, i- and n- Butane, i- and n- Pentane and n- Hexane. The model was developed based on MESH equations, using MATLAB programming tool, as required by MLNG. The depropanizer column model was developed to account for the non-ideality of the mixture by incorporating Redlich-Kwong equation of state in the enthalpy balances. The outputs obtained from the model include vapor and liquid flow profiles, composition profiles and temperature profile of the depropanizer column. The model developed in the study was able to predict the flow profiles, plate composition and temperature to good accuracy. In the depropanizer column, vapor and liquid flow rates, and column temperature decrease from the bottom tray up to top tray. The composition of the desired product (propane) increases ascending the column. The inverse trends occur for other heavier components. "What-If" analysis, which can be used for optimization study, was also carried out on feed flow rate and reflux ratio. Conclusively, a functional model of the MLNG depropanizer column was successfully built.

ACKNOWLEDGEMENT

I would like to extend my heartfelt appreciation to all individuals who had kindly given me assistance and guidance during the completion of this project.

First of all, I would like to express my sincere gratitude to my supervisor, Prof. Dr. V. R. Radhakrishnan for his guidance, constructive advices and encouragement throughout the duration of this project.

Secondly, I would like to extend my profound appreciation to Dr. Abdul Huq M. Abd. Wahhab, a lecturer from Electrical and Electronics Engineering Department of Universiti Teknologi Petronas, for his guidance in numerous aspects of the mathematical modeling.

Thirdly, I would also like to thank Ms. Tan Khang Meei for her help and support in completing this project.

Last but not least, I would like to express my deepest gratitude to my parents, siblings and friends for their constructive support during the whole period of completion of this project.

TABLE OF CONTENTS

LIST OF FIGURES

CHAPTER 1

INTRODUCTION

1.1   BACKGROUND OF STUDY

Malaysia is the world third largest exporter of liquefied natural gas (LNG), after Algeria and Indonesia. The LNG processing plant in Bintulu, Sarawak (LNG1) is owned by Malaysia Liquefied Natural Gas Sdn. Bhd. (MLNG). The plant has an LNG production capacity of 8.1 million metric tons per annum.

Although natural gas consists of primarily methane, it also includes ethane, propane, butane, pentane and hexane and traces of other components. The typical natural gas composition is as shown in Table 1.1. Propane, which is the component of interest in this project, naturally occurs as a gas at atmospheric pressure but can be liquefied if subjected to moderately increased pressure.

Table 1.1 Typical composition of natural gas

Component	Composition
Methane, CH_4	70-90%
Ethane, C_2H_6	0-20%
Propane, C_3H_8	
Butane, C_4H_{10}	
Carbon dioxide, CO_2	0-8%
Oxygen, O_2	0-0.2%
Nitrogen, N_2	0-5%
Hydrogen sulphide, H_2S	0-5%

Source: MLNG

Propane is usually not produced for its own sake, but is a byproduct of two other processes, natural gas processing and petroleum refining. One of the typical steps in natural gas processing is a 4-column distillation system, which separates methane, ethane, propane, butane and pentane sequentially. Propane is obtained from the depropanizer column where propane is separated from higher hydrocarbons such as butane, pentane and hexane.

In the MLNG Depropanizer Column, tagged as C-15-03, propane is separated from butane and other heavier hydrocarbons via distillation process. The liquid exiting from the bottom of the deethanizer column is fed to the depropanizer column. This feed consists of propane, n-butane, iso-butane, n-pentane, iso-pentane and n-hexane. The column overhead product is propane whereas butane and other heavier components are removed as bottom product, to be fed into the debutanizer. Figure 1.1 shows the simplified depropanizer column.
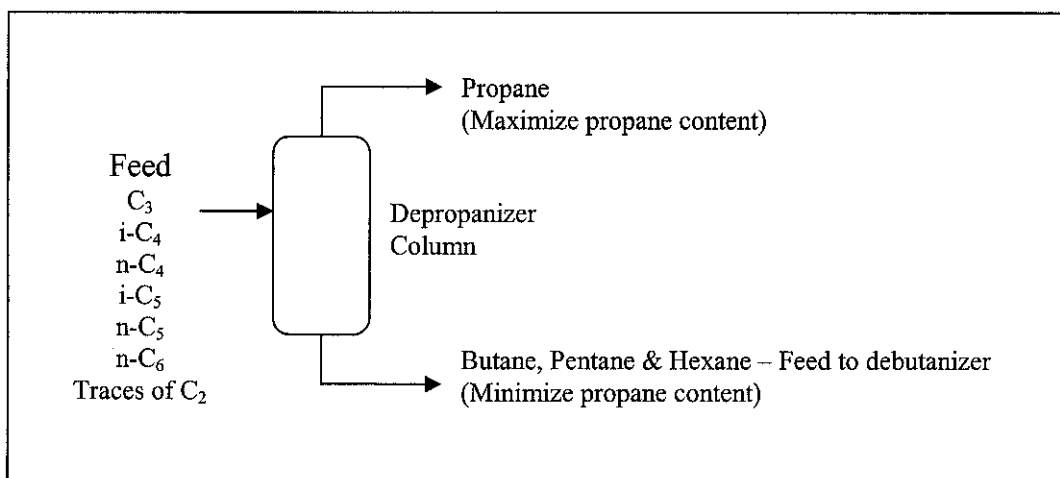
Figure 1.1 Simplified diagram of depropanizer column

A large portion of this product will be exported, which is a valuable source of income for MLNG. Propane is used mainly as fuel, for heating purposes, cooking and as an alternative fuel for vehicles. Over the years, more propane is used in the petrochemical industries as raw material for the building blocks for plastics and fibers. Propane is also used as refrigerant for internal use in the cryogenic systems.

1.3   OBJECTIVE

The main objective of this study is to develop a distillation column model for MLNG depropanizer column by incorporating the non-ideal equation of state in the column model to account for the non-ideal effect of the real fluid mixture. The model is to be built using MATLAB programming tool.

1.4   SCOPE OF STUDY

The necessary data user input for the model was obtained from MLNG. The process feed parameters were obtained from HYSIS simulation that were performed by MLNG personnel. On the other hand, operational parameters were obtained from MLNG actual plant data, which was taken over a period of time when the plant was in smooth operation. MATLAB tool is used to solve physical constraint equations such as material and energy balance equations.

The main part of the project was focused on improving the model developed in previous project papers by seniors. Thermodynamic properties, especially enthalpy, of the real mixture were approximated using non-ideal equation of state to account for the deviation from ideal condition. Non-ideal thermodynamic property model, namely the Redlich-Kwong equation of state, was applied. For real mixtures, values of these thermodynamic properties are computed as functions of temperature, pressure and phase compositions.

The model was built based on the following assumptions:
1. 100% tray efficiency
2. Narrow-boiling feed mixture

4

CHAPTER 2
LITERATURE REVIEW / THEORY

2. LITERATURE REVIEW

This chapter explains the theory of the separation process using distillation as well as the rigorous calculations procedures involved. Furthermore, the method used for computing the thermodynamic properties of non-ideal mixture, which is the Redlich-Kwong equation of state is also explained in detail.

2.1 INTRODUCTION TO DISTILLATION

Distillation is a separation process which is used to separate components of a liquid solution by their differences in boiling point. In other words, separation of components in a liquid mixture via distillation depends on the differences in boiling points of the individual components.

Distillation process exploits the fact that the equilibrium compositions of chemical species across coexisting phases are not equal. Thus, by repeatedly contacting the phases in a countercurrent fashion, it is possible to isolate one or more of the components present in the feed mixture. In a distillation process, an intimate contact is created between the starting mixture and a second phase in order to enhance an effective mass transfer between these two phases. Mass transfer of components then occurs between these two phases. After the mass transfer, the two phases are then separated into two single phases with different compositions of components. Thus, separation of components in a mixture is achieved.

According to Seader (1998, pg 176), a flash is a single-equilibrium stage distillation in which a feed is partially vaporized to give a vapor richer in the more volatile components than the remaining liquid. Rectification distillation, which is distillation with reflux, can be considered to be a process in which a series of flash-vaporization stages are arranged in such a manner that the vapor and liquid products from each stage flow counter currently to each other. The liquid in a stage flows down to the stage below and the vapor from a stage flows upward to the stage above. Hence, in each stage, a vapor stream, V and a liquid stream, L enter, are mixed and equilibrated, and a vapor and a liquid stream leave in equilibrium.

The concentration of the more volatile component, also called light key, is being increased in the vapor going upward and decreased in the liquid going downward. Thus, the top product (distillate) is highly concentrated in the more volatile component. The section of the column above the feed stage is known as the rectifying section. On the other hand, the bottom product (bottoms) is highly concentrated in the less volatile component (heavy key). This section is called stripping section.
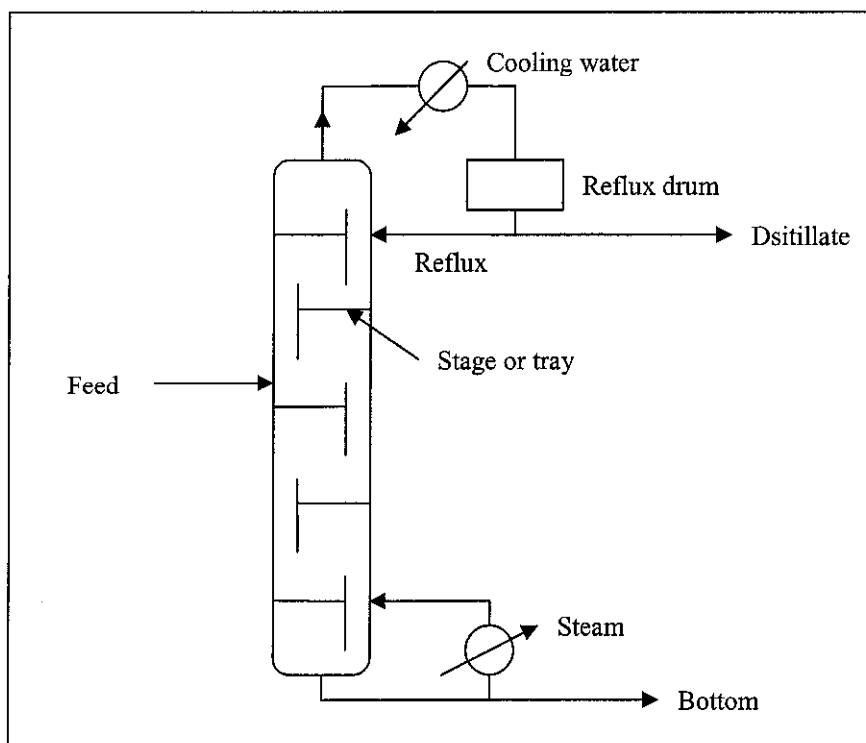
Figure 2.1 Schematic drawing of a distillation column.

2.1.1 Multicomponent Distillation

The depropanizer column in MLNG plant is a multicomponent distillation column. The feed contains propane (C_3) to octane (C_8), where heavier components (above C_6) are found in traces. The light key is propane, which is the desired product of depropanizer. Iso-butane, which is the heavy key, and the other heavier products, which are heavy non-keys, will be removed as bottom products.

2.2 EQUILIBRIUM STAGE CONCEPT

Wankat (1988, pg. 1) stated that the *equilibrium stage* concept is applicable when the process can be constructed as a series of stages where vapor and liquid phases are contacted and then separated. The two separated phases are assumed to be in equilibrium with each other. The key assumption utilized in developing the column model is that the vapor and liquid streams leaving each stage are in equilibrium.

The distillation process is based on equilibrium stage concept. In distillation, both liquid and vapor phases are in contact. Liquid molecules continually vaporize whereas vapor molecules continually condense. At equilibrium, the rate at which each species condenses equals the rate at which it vaporizes. Thus, there is no change in the composition in both vapor and liquid phases. (Wankat, 1998, pg. 10) When it is in equilibrium, both vapor and liquid temperature and pressure are the same, and they are present in same mole fractions.

One way to represent equilibrium data is to define a distribution coefficient (K-value) where K-value is defined as

$$K_i = y_i/x_i \qquad \text{(Eq. 1)}$$

where y_i = Vapor mole fraction of component i

x_i = Liquid mole fraction of component i

2.3   RIGOROUS COLUMN SIMULATION

Rigorous calculation procedures are more accurate in evaluating the thermodynamics and operating conditions in the distillation column. The solutions are obtained by solving material balance, energy balance and equilibrium relations at each stage. These relations are nonlinear algebraic equations. Thus, solution procedures are relatively difficult and tedious. However, rigorous methods are readily available for computer-solution of equilibrium-based models.

2.3.1   MESH Equations

A schematic diagram of a single equilibrium stage is shown in Figure 2.2. Subscript j refers to the tray number.
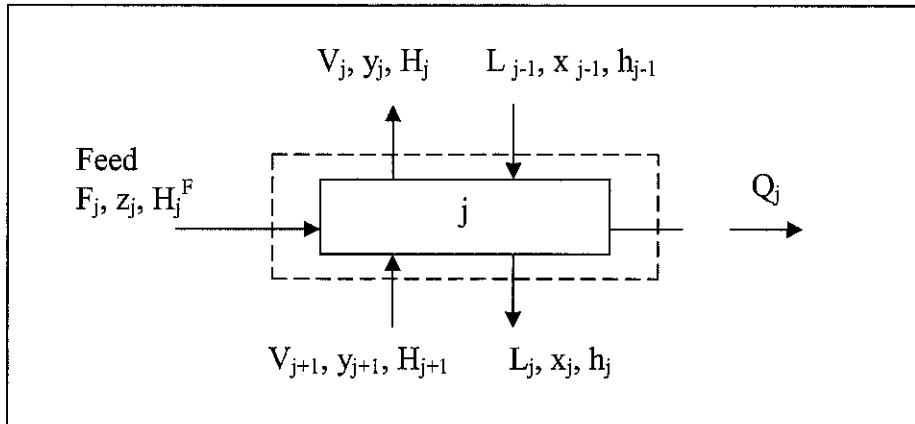
Figure 2.2   Simplified schematic diagram of a stage in a column.

The equations that model equilibrium stages have been termed the MESH equations. According to Taylor (1993, p 385), the M equations are the **M**aterial balance equations.

$$M_j = V_j + L_j - V_{j+1} - L_{j-1} - F_j = 0 \qquad (\text{Eq. 2})$$

The E equations are the phase **E**quilibrium relation for each component.

$$E_{i,j} = K_{i,j}x_{i,j} - y_{i,j} = 0 \qquad (\text{Eq. 3})$$

The S equations are the mole fraction *S*ummation (one for each stage) equations.

$$S_j^V = \sum y_{i,j} - 1 = 0 \qquad \text{(Eq. 4)}$$

$$S_j^L = \sum x_{i,j} - 1 = 0 \qquad \text{(Eq. 5)}$$

The H equations are the ent*H*alpy balances (one for each stage)

$$H_j = V_j H_j + L_j h_j - V_{j+1} H_{j+1} - L_{j-1} h_{j-1} - F_j H_j^F + Q_j = 0 \qquad \text{(Eq. 6)}$$

where H_j and h_j are equations of the vapor and liquid streams leaving the jth stage; H_j^F is the enthalpy of the feed stream.

MESH-equations represent a set of n. (2k + 3) equations where n denotes the number of stages and k the number of components. (J. G. Stichmair, 1998, p.172). Thus, the separation of six-component mixture in a 47 equilibrium stages column gives a system of 705 equations. In addition, complex functions for vapor-liquid equilibrium ratios, K and for vapor and liquid enthalpies, H_j and h_j, are required.

A wide variety of iterative solution nonlinear algebraic equations are available. The earliest manual methods for solving the MESH equations were those of Lewis and Matheson (LM) and Thiele and Geddes (TG). In both methods, the equilibrium stage equations are solved one by one by using tearing techniques and suffer from numerical difficulties that can prevent convergence in certain cases. (Perry et al., 1997) Stage-by stage method groups all MESH equations at each stage and solved from stage to stage.

For equation-to-equation method, however, the MESH equations are grouped and solved by type, instead of stage by stage. All mass and energy balances for one component are grouped and solved simultaneously. According to Seader (1998), current practice is mainly based on equation-to-equation method, such as Bubble Point (BP) method and Sum-Rates (SR) method. The equation-to-equation method derivation and explanation have been detailed out by Wankat (1988, p.251). A brief description of the general procedures is included in Section 2.3.2 below.

2.3.2 Equation to Equation Method

For distillation that involves species with a relatively narrow range of vapor-liquid equilibrium ratios (K values), Wang and Henke (1966, p. 155-163) had developed an effective solution procedure called the Bubble Point (BP) method. In this method, the modified M equations are solved separately for each component by tridiagonal matrix. All the other equations are partitioned and solved sequentially.

To start the calculations, initial guess values of liquid flow rate (L), vapor flow rates (V) and temperature (T) for every tray j has to be made. Initial estimate of vapor-rate profile is obtained based on the assumption of constant molal overflow (CMO). Temperature guesses are obtained by assuming a linear variation of temperature between reboiler and condenser. The calculations of stages are carried out from bottom to top. Tray 1 is partial reboiler and the total condenser is labeled as tray N. For a general stage j within the column (Please refer to Figure 2.2), the mass balance for any component is

$$V_j y_j + L_j x_j - V_{j-1} y_{j-1} - L_{j+1} x_{j+1} = F_j z_j \qquad \text{(Eq.7)}$$

The vapor compositions, y_j and y_{j-1}, can be replaced using the equilibrium expressions:

$$y_j = K_j x_j \qquad \text{(Eq.8)}$$

Liquid compositions, x_j and x_{j+1} can also be replaced with

$$x_j = {l_j}/{L_j} \quad ; \quad x_{j+1} = {l_{j+1}}/{L_{j+1}} \qquad \text{(Eq.9)}$$

where l_j and l_{j+1} are liquid component flow rates.

By replacing the unknown vapor and liquid compositions with known parameters, the following equation can be developed from (Eq. 7).

$$\left[\frac{-V_{j-1}K_{j-1}}{L_{j-1}}\right]l_j - 1 + \left[1 + \frac{V_jK_j}{L_j}\right]l_j + (-1)l_{j+1} = F_jz_j \qquad \text{(Eq. 10)}$$

(Eq.10) can be written in the general form of

$$A_jl_{j-1} + B_jl_j + C_jl_{j+1} = D_j \qquad \text{(Eq.11)}$$

Linear matrix equations can be developed to solve for liquid component flow rates. The matrix form used in this project is the tridiagonal matrix (Eq.12).

$$\begin{bmatrix} B_1 & C_1 & 0 & 0 & 0 & \bullet & 0 & 0 & 0 \\ A_2 & B_2 & C_2 & 0 & 0 & \bullet & 0 & 0 & 0 \\ 0 & A_3 & B_3 & C_3 & 0 & \bullet & 0 & 0 & 0 \\ \bullet & \bullet & \bullet & \bullet & \bullet & \bullet & \bullet & \bullet & \bullet \\ 0 & 0 & 0 & 0 & 0 & \bullet & A_{N-1} & B_{N-1} & C_{N-1} \\ 0 & 0 & 0 & 0 & 0 & \bullet & 0 & A_N & B_N \end{bmatrix} * \begin{bmatrix} l_1 \\ l_2 \\ l_3 \\ \bullet \\ l_{N-1} \\ l_N \end{bmatrix} = \begin{bmatrix} D_1 \\ D_2 \\ D_3 \\ \bullet \\ D_{N-1} \\ D_N \end{bmatrix} \qquad \text{(Eq.12)}$$

Liquid component flow rates of each component at each tray is solved by inverting the matrix (Eq.12) using the Thomas algorithm.

After the liquid flow rates are determined, the assumed temperature must be corrected using bubble-point calculations on each tray. Theta method is used. As detailed in Wankat (1988, p. 257), this method first adjusts the component flow rates so that the specified distillate flow rate is satisfied. Then mole fractions are determined and bubble-point calculations on each tray are done to calculate new temperatures. Theta method defines a value of theta that forces the equation (Eq.13) to be satisfied. Theta value is determined through Newtonian convergence procedure [(Eq.14) and (Eq. 15)].

$$D_{spec} = \sum_{i=1}^{C}\left(\frac{Fz_i}{1 + \theta(Bx_{i,bot} / Dx_{i,dist})_{calc}}\right) \qquad \text{(Eq.13)}$$

11

$$f(\theta) = \sum_{i=1}^{C}\left(\frac{Fz_i}{1+\theta(Bx_{i,bot}/Dx_{i,dist})_{calc}}\right) - D_{spec} \qquad (Eq.14)$$

$$\theta_{N+1} = \theta_N + \frac{f(\theta_N)}{\sum_{i=1}^{C}\left[\dfrac{Fz_i(Bx_{i,bot}/Dx_{i,dist})_{calc}}{(1+\theta_N(Bx_{i,bot}/Dx_{i,dist})_{calc})^2}\right]} \qquad (Eq.15)$$

After convergence of the temperature loop, the liquid and vapor flow rates, L and V have to be corrected using energy balances. For a general stage j (Please refer to Figure 2.2), the energy balance is

$$L_j h_j + V_j H_j = V_{j-1}H_{j-1} + L_{j+1}h_{j+1} + F_j h_{Fj} + Q_j \qquad (Eq.16)$$

Liquid flow rates are derived from mass balance around the bottom of the column:

$$L_j = V_{j-1} + B - \sum_{k=1}^{j-1}F_k \qquad (Eq.17)$$

By substituting (Eq.17) into (Eq.16), (Eq.16) becomes

$$(h_j - H_{j-1})V_{j-1} + (H_j - h_{j+1})V_j = F_j h_{Fj} + Q_j + B(h_{j+1} - h_j) + (\sum_{k=1}^{k-1}F_k)h_j - (\sum_{k=1}^{j}F_k)h_{j+1} \quad . \qquad (Eq.18)$$

Similarly, equation (Eq.18) can be generalized as

$$A_{E,j}V_{j-1} + B_{E,j}V_j = D_{E,j} \qquad (Eq.19)$$

The coefficients A_E, B_E and D_E can be obtained by comparing equations (Eq.19) and (Eq.16). All the values are put in matrix form, as shown in (Eq.20).

$$
\begin{bmatrix}
B_{E1} & 0 & 0 & 0 & \bullet & & & & \\
A_{A2} & B_{E2} & 0 & 0 & \bullet & & & 0 & \\
0 & A_{E3} & B_{E3} & 0 & \bullet & & & & \\
\bullet & \bullet & \bullet & \bullet & \bullet & \bullet & \bullet & \bullet & \bullet \\
0 & 0 & 0 & 0 & \bullet & 0 & A_{EN-1} & B_{EN-1} & 0 \\
0 & 0 & 0 & 0 & \bullet & 0 & 0 & A_{EN} & B_{EN}
\end{bmatrix}
*
\begin{bmatrix}
VE_1 \\ VE_2 \\ VE_3 \\ \bullet \\ VE_{N-1} \\ VE_N
\end{bmatrix}
=
\begin{bmatrix}
D_{E1} \\ D_{E2} \\ D_{E3} \\ \bullet \\ D_{EN-1} \\ D_{EN}
\end{bmatrix}
\qquad \text{(Eq.20)}
$$

The matrix (Eq.20) can be inverted to obtain the vapor flow rates, V_j. To determine the coefficients for A_E and B_E, the enthalpies leaving each stage have to calculated. The computation of enthalpies will be discussed in Section 2.5.

For this project, the column operates under adiabatic condition. Thus, $Q_j = 0$. The condenser requirement is determined from balances around the total condenser:

$$
Q_N = V_{N-1}(h_D - H_{N-1}) = D(1 + \frac{L}{D})(h_D - H_{N-1}) \qquad \text{(Eq.21)}
$$

The reboiler heat load can be calculated from overall energy balance:

$$
Q_1 = Dh_D + Bh_B - \sum_{j=1}^{N}(F_j h_{Fj}) - Q_N \qquad \text{(Eq.22)}
$$

The liquid flow rates can be determined from mass balance (Eq.19). All the new liquid and vapor flow rates are compared to the values used for previous convergence of mass and temperature loop. If

$$
\left| \frac{L_{j,new} - L_{j,old}}{L_{j,new}} \right| < \varepsilon \qquad and \qquad \left| \frac{V_{j,new} - V_{j,old}}{V_{j,new}} \right| < \varepsilon \qquad \text{(Eq.23)}
$$

for all stages, then the calculation has converged. For computer calculation, an ε of 10^{-3} to 10^{-5} is appropriate.

13

2.4 EQUIBRIUM DISTRIBUTION COEFFICIENT

In general, the equilibrium distribution coefficient, K_i, depends on temperature, pressure and composition. However, for many systems, the K values are approximately independent of composition. For aliphatic hydrocarbon mixtures in the $C_1 - C_{10}$ range, K values can be determined from a set of monographs prepared by DePriester. (Doherty and Malone, 2001, p. 58) The DePriester charts have been fit to McWilliams's regression equation (Eq.24).

$$\ln K = \frac{a_{T1}}{T^2} + \frac{a_{T2}}{T} + a_{T6} + a_{p1} \ln p + \frac{a_{p2}}{p^2} + \frac{a_{p3}}{p} \qquad \text{(Eq.24)}$$

where T = temperature, °R

p = pressure, psia

The constants a_{T1}, a_{T2}, a_{T6}, a_{p2} and a_{p3} are tabulated in Table 2.1. Equation Eq. 24 is valid from -70 °C (365.7 °R) to 200 °C (851.7 °R) and for pressures from 101.3 kPa (14.69 psia) to 6000 kPa (870.1 psia) (Wankat, 1988, p.23-24). In MLNG, the operating pressures for both condenser and reboiler used are in the order of 11 to 20 bars. Therefore, the use of the McWilliam's regression equation is valid.

Table 2.1 Equation Constants for Components in Eq. 24

Compounds	a_{T1}	a_{T2}	a_{T6}	a_{p1}	a_{p2}	a_{p3}
Propane	-970688.57	0	7.15059	-.76984	0	6.90224
Isobutane	-1166846	0	7.72668	-.92213	0	0
n-butane	-1280557	0	7.94986	-.96455	0	0
i-pentane	-1481583	0	7.58071	-.93159	0	0
n-pentane	-1524891	0	7.33129	-.89143	0	0
n-hexane	-1778901	0	6.96783	-0.84634	0	0

Source: McWilliams (1973)

2.5 THERMODYNAMIC PROPERTIES

Thermodynamics properties play a major role in separation operations, particularly with respect to energy requirements and phase equilibrium. For this project, the enthalpy property of both vapor and liquid phases were studied extensively.

2.5.1 Equation of State

Equations of state (EOS) attempt to describe the relationship between temperature (T), pressure (P), and volume (v) for a given substance or a mixture. The ideal gas law is one of the simplest equations of state. Although reasonably accurate for gases at low pressures and high temperatures, it becomes increasingly inaccurate at higher pressures and lower temperatures.

The ideal gas equation cannot describe real fluids in most situations because the fluid molecules themselves occupy a finite volume and they exert forces of attraction and repulsion on each other. Numerous equations of state have been developed on the basis of molecular thermodynamics. These include van der Waals, Redlich-Kwong and Peng Robinson equation.

Seader (1998, p.42) stated that ideal gas equations apply only at near-ambient pressure, up to about 50 psia (3.34 bar) MLNG depropanizer column operates in the range of 11 to 20 bars. This range of pressure is significantly above the limitation of ideal equations. Therefore, in order to predict the enthalpy properties of the gas and liquid mixtures more accurately, the equation of state is employed in the column modeling.

The generalized equation in describing the P-V-T behavior of a fluid is given as follow:

$$Pv = ZRT \qquad \text{(Eq.25)}$$

where Z = Compressibility factor

15

2.5.2 Redlich-Kwong Equation

Introduced in 1949, the Redlich-Kwong equation of state, also known as R-K equation, was a considerable improvement over the van der Waals equation due to the temperature dependency for the attraction parameter.

Theoretically, the Redlich-Kwong equation is adequate for calculation of gas phase properties when the ratio of the pressure to the critical pressure is less than about one-half of the ratio of the temperature to the critical temperature. However, one drawback of the R-K equation is that it performs poorly with respect to the liquid phase. Thus, it is not the best EOS to be used for accurately calculating vapor-liquid equilibria.

In this project, the Redlich-Kwong equation was adapted due to its simplicity. The Redlich-Kwong equation also gives accurate values for gases, and reasonable approximations for saturated liquids and vapors.

The Redlich-Kwong Equation of State:

$$P = \frac{RT}{V-b} - \frac{a}{\sqrt{T}V(V+b)}$$

(Eq.26)

$$a = \frac{0.42748R^2T_c^{2.5}}{P_c}$$

(Eq.27)

$$b = \frac{0.08664RT_c}{P_c}$$

(Eq.28)

where P = Pressure (Pa)

V = Molar volume, the volume of 1 mole of gas or liquid

T = Temperature (K)

R = Ideal Gas constant (8.31451 J/mol·K)

The empirical constants (parameters a and b) are evaluated in terms of the critical constants by applying the critical point conditions. The critical constants for use in the evaluation of the empirical constants are defined as follows and tabulated in Table 2.2.

P_c = Critical pressure, bar

T_c = Critical temperature, K

Table 2.2: Critical Constants for Evaluating Empirical Constants in Eq. 27 and Eq. 28.

Compounds	Critical pressure, P_c (bar)	Critical temperature, T_c (K)
Propane	42.5	369.8
Isobutane	36.5	408.2
n-butane	38.0	425.2
i-pentane	33.9	460.4
n-pentane	33.7	469.7
n-hexane	40.7	553.5

Source: Winnick (1997)

The equation of state must be general enough to apply to liquid and vapor. Yet it must not be too complex that it presents analytical difficulties in application. Two parameter cubic equations of state coupled with the classical van der Waals mixing rules are probably the most extensively used modeling tool for the Vapor Liquid Equilibria (VLE) of hydrocarbon mixtures.

Cubic equations are characterized by predicting three real values of the volume in the vapor-liquid region. When a homogenous liquid phase is in equilibrium with a vapor, T and P are the same in both phases. In such a case when the EOS selected is solved at selected T, P and composition, three volume roots are obtained at temperature less than the critical temperature.

The smallest volume corresponds to the liquid whereas the largest value corresponds to the vapor. The intermediate value has no physical significance.

17

Equation of state are extended to mixtures by replacing pure component parameters with mixture parameters. (Khoury, 2000, p. 18). To apply the R-K equation to mixtures, such as the ones in the depropanizer column, mixing rules are used to average the constants a and b for each component in the mixture. According to Seader (1998, p. 56), the recommended rules for vapor mixtures of C components are:

$$a = \sum [\sum y_i \, y_j \, (a_i \, a_j)^{0.5}] \qquad \text{(Eq.29)}$$
$$b = \sum y_i \, b_i \qquad \text{(Eq.30)}$$

2.6 ENTHALPY PROPERTIES

The energy balances are required in the depropanizer column modeling project. Thus, both vapor and liquid enthalpies are calculated. To improve the accuracy of the predicted enthalpies, the residual enthalpy was calculated. Non-ideal equation of state, which is the Redlich-Kwong EOS was employed.

2.6.1 Ideal Enthalpy

As mentioned earlier, the simplest model for VLE properties is the ideal gas equation. For an ideal gas solution, the vapor molar enthalpy, h_v, can be computed by

$$h_v = \sum_{i=1}^{C} y_i h_{i\,v}^{o} \qquad \text{(Eq.31)}$$

where h_v^0 = Ideal gas species molar enthalpy

Ideal gas species molar enthalpy h_v^0 is given in the following equation:

$$h_v^o = \int_{T_0}^{T} C_{pv}^o dT = \sum_{k=1}^{4} a_k \frac{(T^k - T_0^k)}{k} \qquad \text{(Eq.32)}$$

where the constants a_k depend on the species.

$$\frac{C_p^o}{R} = a + bT + cT^2 + dT^{-2} \qquad \text{(Eq.33)}$$

where T = Temperature (K) and R = $8.314e^{-3}$ kJ/mol.K.

The values for the coefficients of the equation are tabulated in Table 2.3.

Table 2.3 Coefficients for ideal gas enthalpy calculations

Compound	a	b	c	d
Propane	1.212768	0.028782	-0.0000088	0
i-butane	1.67674	0.037849	-0.000012	0
n-butane	2.240853	0.036368	-0.000011	0
i-pentane	2.423523	0.046088	-0.000015	0
n-pentane	2.974049	0.04451	-0.000014	0
n-hexane	3.762599	0.052548	-0.000016	0

Source: Perry's et. al. (1997)

For an ideal liquid solution, the liquid molar enthalpy, h_L is given as,

$$h_L = \sum_{i=1}^{C} x_i (h_{iv}^o - \Delta h_{i,vap}) \qquad \text{(Eq.34)}$$

$\Delta h_{i,vap}$ is the heat of vaporization for a pure component. The values for Δh_{vap} (J/kmol) can be computed by using the following equation.

19

$$\Delta h_{vap} = C1 * (1 - T_r)^{C2 + C3*T_r + C4*T_r*T_r} \qquad \text{(Eq.35)}$$

The data for the coefficients in equation (Eq.35) are tabulated as below:

Table 2.4 Coefficients for calculating heat of vaporization

Compound	C1 x 1E-07	C2	C3	C4	T_{max} (K)
Propane	2.9209	0.78237	-0.77319	0.39246	369.83
i-butane	3.1667	0.3855	0	0	408.14
n-butane	3.6238	0.8337	-0.82274	0.39613	425.12
i-pentane	3.7700	0.3952	0	0	460.43
n-pentane	3.9109	0.38681	0	0	469.7
n-hexane	4.4544	0.39002	0	0	507.6

Source: Perry's Chemical Engineers' Handbook, p.2-156 (1999)

2.6.2 Residual Enthalpy

The properties of real gas phase were calculated by quantifying the departure of the real gas from that of the ideal gas at the same temperature and pressure. These departures are known as residual properties. For a temperature-dependent enthalpy equation, both vapor and liquid phase properties can be derived in a consistent manner by applying the classical integral equations of thermodynamics.

At a given temperature and composition, the mixture enthalpy equation for a non-ideal gas is expressed as:

$$h_v = (h - h^0_v) = Pv - RT - \int_\infty^v [P - T(\partial P/\partial T)_v] \, dv \qquad \text{(Eq.36)}$$

When the Redlich-Kwong (R-K) equation is substituted into the equation, the following result for the vapor phase equation is obtained. (Seader, 1998, p. 59)

$$h_v = \Sigma\ (y_i h^0_{iv}) + RT\ [\ Z_v - 1 - 3A/2B\ \ln\ (B/Z_v)\ ] \qquad\qquad (Eq.37)$$

Note that the first term in the enthalpy equation, $\Sigma\ (y_i h^0_{iv})$, is the ideal molar enthalpy. According to Seader (p. 59), the results for the liquid phase are identical if y_i and Z_v are replaced by x_i and Z_L, respectively. The liquid phase form of (Eq.37) accounts for the enthalpy of vaporization, $\Delta h_{i,vap}$, because the R-K equation of state are continuous functions in passing between vapor and liquid regions.

$$h_L = \Sigma\ (y_i h^0_{iv}) + RT\ [\ Z_L - 1 - 3A/2B\ \ln\ (B/Z_L)\ ] \qquad\qquad (Eq.38)$$

If the R-K equation is expanded to obtain a common denominator, a cubic equation in v is obtained. By combining the R-K equation (Eq.26) together with the generalized equation (Eq.25), the v value is eliminated from the equation, giving the R-K equation in the form of its compressibility factor, Z.

The Z form of the R-K equation is given as the following equation:

$$Z^3 - Z^2 + (A - B - B^2)Z - AB = 0 \qquad\qquad (Eq.39)$$

where $A = \dfrac{aP}{R^2 T^2}$

$B = \dfrac{bP}{RT}$

By solving for the roots of (Eq.39), the value of Z can be obtained. The smallest root corresponds to the liquid phase (Z_L) whereas the largest root corresponds to the vapor (Z_V). Having obtained A, B and Z, these values are then substituted into (Eq.37) to solve for h_v and h_L.

CHAPTER 3

METHODOLOGY / PROJECT WORK

3.   METHODOLOGY

The chapter explains the methodology and the scope of work carried out in the project work. A concise problem statement was first defined. The fundamental concepts of the distillation process were then studied. The modeling equations for the system were formulated and organized into manageable equations. Technical computing was then carried out. The results obtained from the model were then analyzed. The methodology is simplified in Figure 3.1 below.

```
┌─────────────────────────────────────┐
│        Problem Definition            │
└─────────────────────────────────────┘
                  │
                  ▼
┌─────────────────────────────────────┐
│        Literature Review             │
└─────────────────────────────────────┘
                  │
                  ▼
┌─────────────────────────────────────┐
│   Modeling Equations Formulation     │
└─────────────────────────────────────┘
                  │
                  ▼
┌─────────────────────────────────────┐
│  Mathematical Equations Developing   │
└─────────────────────────────────────┘
                  │
                  ▼
┌─────────────────────────────────────┐
│           Computation                │
└─────────────────────────────────────┘
                  │
                  ▼
┌─────────────────────────────────────┐
│      Interpretation of Results       │
└─────────────────────────────────────┘
```
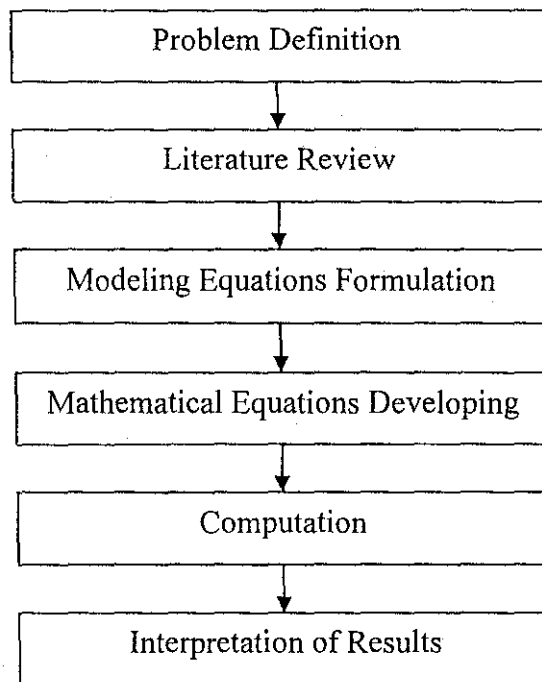
Figure 3.1 Methodology of Project Work

3.1   PROCEDURE IDENTIFICATION

3.1.1   Problem Definition

Clear and concise definition of the problem statement is very important in the modeling of the depropanizer column project.

Once the problem statement had been identified, necessary data were gathered. These data were required to formulate the initial estimates of for model. The input information includes plant daily operational output worksheet of the depropanizer column on August 2003 and HYSYS simulation data from MLNG. The input data used was approximately the average of available plant data, as shown in table below.

Table 3.1 Geometric and Operational Data of Depropanizer Column

	Parameters	
	Feed flow rate	626.4 tons/day
	Feed composition	
	Propane	0.2094
	Iso-butane	0.1559
	n-Butane	0.2327
FEED	Iso-pentane	0.1362
	n-Pentane	0.0881
	n-Hexane	0.1777
	Pressure	18.56 bar
	Temperature	95°C
	Reflux ratio	8
	Distillate flow rate	100.2 tons/day
	Recovery of propane in distillate	0.98
OPERATIONAL	Condenser temperature	45 °C
	Condenser pressure	14.26 bar
	Reboiler temperature	100 °C
	Number of stages	47
GEOMETRIC	Feed stage	16

Source: MLNG

23

The scope of the modeling work was specified at this stage by stating the assumptions employed for the modeling work. The significant assumptions made were:

1. 100% tray efficiency.
2. Narrow boiling feed mixture.

3.1.2 Literature Review

Research on distillation concept as well as the established mathematical modeling methods was conducted. Reports from seniors who had completed similar projects were studied, apart from other relevant reference books. Reports and various related materials were studied in order to obtain sound understanding on the project background. This provides understanding on the rigorous simulation methods of distillation process and also on vapor-liquid equilibrium.

3.1.3 Formulation of Modeling Equations

The appropriate equations required to model the column were identified. MESH equations were used to solve multicomponent distillation problems. The procedure used in modeling the column is based on Bubble-Point method. For the first part of the model, bubble–point calculations and a relatively simple matrix approach, called theta method were used for temperature convergence. The second part of the model was carried to correct the liquid and vapor flow rates using energy balances by incorporating the Redlich-Kwong equation of state. The key equations for the calculations are presented in Chapter 2.

3.1.4 Mathematical Equations Organization

When all the required mathematical relations were assembled, they were arranged into a solution strategy. There were generally two parts to the model. In the first part of the model, the overall mass balance of the depropanizer column was performed. Then, the

pressure and first estimate of temperature for each tray of the column were determined by the method of linear variation. Next, the equilibrium ratio of each tray was calculated based on the pressure and initial guess of temperature. The component mass balances were solved in matrix form to obtain the vapor and liquid flow rates. The liquid and vapor mole fractions for each component were determined and corrected using theta convergence method. With the corrected values of liquid mole fraction at each tray, the new temperatures were calculated with bubble-point calculations. Corresponding to these temperatures, new K values were determined and they were used to iterate the component mass balances until a converged temperature profile, where deviation of theta value is within the range of 0.00001.

After convergence of temperature loop, the liquid and vapor flow rates were corrected using energy balances. At this level, the assumption of constant molal overflow (CMO) was nullified. To perform this, the vapor and liquid enthalpies were calculated based on Redlich-Kwong EOS equations [(Eq.35) and (Eq.36)]. The parameters required in the enthalpies calculation were determined prior to the enthalpy calculations. By solving the balances around the total condenser, the condenser requirement was determined (Eq.21). Similarly, the reboiler heat load was calculated from overall energy balance (Eq.22).

As vapor flow rate at condenser is zero, thus, the vapor flow rates at each tray were determined by solving the energy balances using the simple solution of algebraic equations, instead of using the method of matrix inversion. The calculation procedure is detailed in Appendix A. The liquid flow rates were then determined from mass balance (Eq.17) in Chapter 2. These new liquid and vapor flow rates were compared to the values used for the previous convergence of mass balances and temperature loop. The comparison was based on equation (Eq.23).

If ε is less than 0.001, the new vapor and liquid flow rates were converged. If the values had not converged, the new values of vapor and liquid flow rates were directly used in the mass balance and temperature loop for the next trial. This approach is known as direct substitution.

When convergence was reached, the calculation loop was considered completed. The mass balances, equilibrium relationships, and energy balance developed for the modeling had all been satisfied. The solution gives the liquid and vapor mole fractions, flow rates and the temperature on each tray.

The calculation procedures explained above is outlined in Figure 3.2.

3.1.5 Computation

Several types of computation can be employed to solve for process simulation problems. MATLAB version 6.1 was selected as the programming tool to be used. The reason of choosing this programming tool will be discussed in the second part of this chapter.

Before proceeding with the actual programming, an algorithm for the programming solution was developed. A pseudo code was also created. Both the algorithm and pseudo code were prepared based on the flow chart in Figure 3.2. The actual coding of the algorithm was then carried out in the MATLAB ordinary text file, called M-file. All the MATLAB codes are presented in Appendix B.

After the coding of the algorithm was completed, the program did not run correctly for the first time. Therefore, debugging process is required. In computer terminology, an error in a program is called a *bug*. The process of detecting and correcting such errors is called debugging. Through the debugging process, any problem with the program codes were isolated and fixed, one by one. The syntax errors (typing errors) and run-time errors of the codes were then corrected successfully.

3.1.6 Interpretation of Results

The results obtained from the depropanizer column model include vapor and liquid flow, temperature and composition profiles. The results were interpreted to justify the

process trend with the theory. "What If" analysis was performed to test the feasibility of model developed. This analysis was done by varying the feed flow rate and reflux ratio while keeping all the other parameters constant. All the parameter profiles from the model with variation of inputs were analyzed and justified. The justifications for each profile will be discussed in Chapter 4.

3.2   TOOLS REQUIRED

Several programming tools are available for developing the MLNG depropanizer column model such as HYSYS, FORTRAN, C++ as well as MATLAB. MATLAB programming tool was selected due to various reasons.

MATLAB stand for **Matrix Laboratory**. MATLAB is a powerful computing system for handling calculations involved in scientific and engineering problems. Mathematical modeling equations are expressed in familiar mathematical notation. MATLAB is based on the mathematical concept of a matrix. Besides common matrix algebra operations, MATLAB offers array operations that allow one to quickly manipulate sets of data in a wide variety of ways. These features allow users to solve many technical computing problems, especially those with matrix and vector formulations, much faster than by using a scalar non-interactive programming language such as the FORTRAN. Since depropanizer column model was built based on MESH equations that made extensive use of matrices in the size of 47 x 47, MATLAB is the best programming tool.

Furthermore, by using MATLAB, depropanizer column model can be built from scratch, using mathematical and chemical engineering principles. This not only enables users to study fundamental concepts and principles of multicomponent distillation, but also enables modification of the model to be carried out easily.
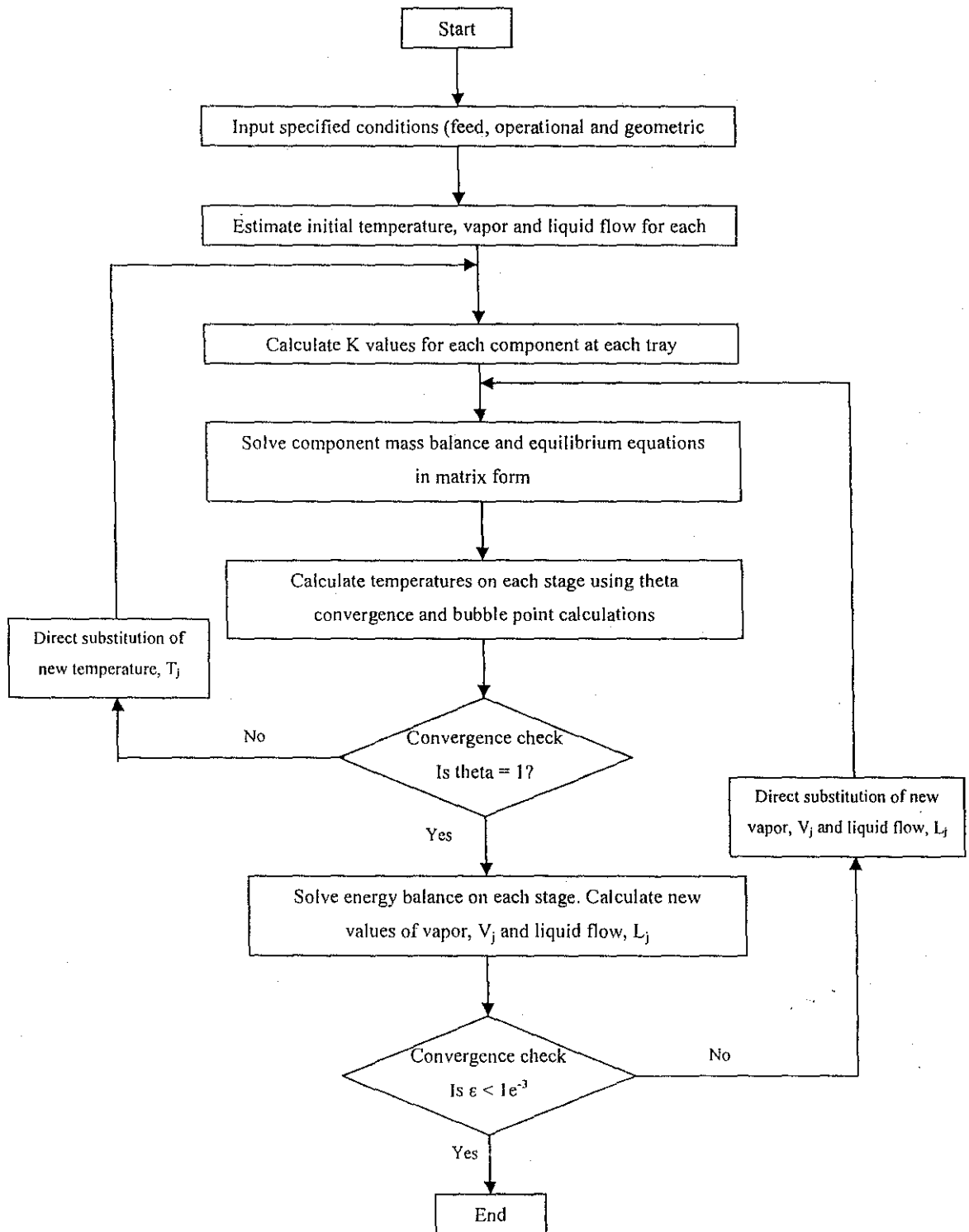
27

Start

Input specified conditions (feed, operational and geometric

Estimate initial temperature, vapor and liquid flow for each

Calculate K values for each component at each tray

Solve component mass balance and equilibrium equations
in matrix form

Calculate temperatures on each stage using theta
convergence and bubble point calculations

Direct substitution of
new temperature, T_j

Convergence check
Is theta = 1?

No

Yes

Direct substitution of new
vapor, V_j and liquid flow, L_j

Solve energy balance on each stage. Calculate new
values of vapor, V_j and liquid flow, L_j

Convergence check
Is $\varepsilon < 1e^{-3}$

No

Yes

End

Figure 3.2 Flow chart of program logic

Adapted from Wankat (1988, p. 252)

CHAPTER 4

RESULTS AND DISCUSSION

4. RESULTS and DISCUSSION

This chapter gives explanations on the results obtained from the depropanizer column model as well as from the "What-If" analysis. Problems encountered and potential solutions for future work are also included.

4.1   PROFILES FOR DEPROPANIZER COLUMN

There are three main outputs obtained from the column model: vapor and liquid flow profiles, vapor and liquid composition profiles and temperature profiles. For all the profiles discussed below, tray 1 refers to the reboiler and tray 47 refers to the condenser. The trays are numbered bottom up.

4.1.1   Vapor and Liquid Flow Profiles

The vapor and liquid flow rates on each tray is an important result obtained from the model. The flow profiles obtained from the model is as shown in Figure 4.1. The figure shows the flow profiles at each tray of the column for both constant molar overflow (CMO) assumption model as well as the improved model. With constant molar overflow assumption, the vapor and liquid flow rates are constant at the stripping and rectifying section of the column. However, when this assumption is nullified, the converged vapor and liquid flow rates vary from tray to tray.
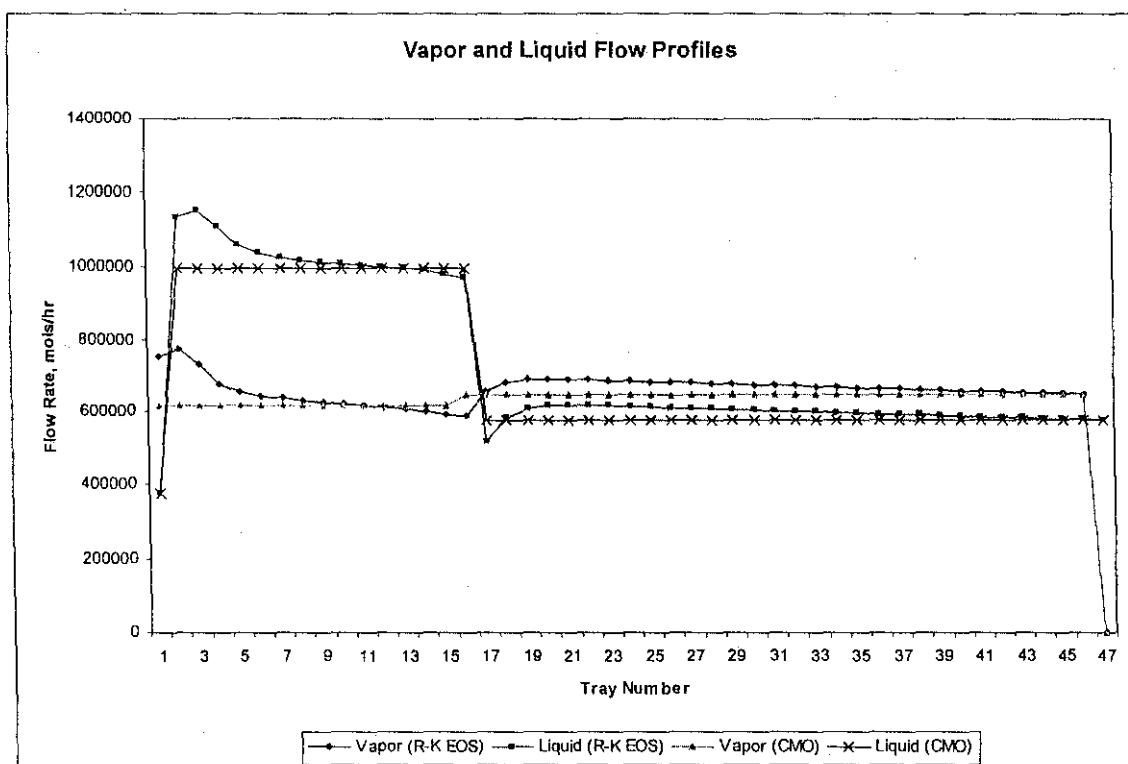
Vapor and Liquid Flow Profiles

Figure 4.1 Flow rate profiles for MLNG depropanizer column

From Figure 4.1, the flow profiles can be generally divided into two portions: above feed tray (rectifying section) and below feed tray (stripping section). The thermal condition of the feed determines the difference between the vapor and liquid flow rates in the two sections of the column. The vapor flow rates do not change as much in the two sections compared to the liquid flow rates.

The liquid flow rate at the stripping section is greater than that at the rectifying section by approximately the feed flow rate. This is because the feed quality is 92.91% liquid, which is near bubble-point (almost saturated). Since the feed enters at almost saturated liquid condition, the vapor flow rate changes only slightly across the feed tray and remains almost constant. Correspondingly, the liquid flow rate decreases across the feed tray by an amount equal to the feed rate.

At the stripping section, both converged vapor and liquid flow rates decrease from bottom trays to feed tray.

The model developed applies the non-ideal gas equation in order to account for non-ideality of the mixture. Figure 4.2 and 4.3 show the vapor and liquid flow rates for both ideal mixture and non-ideal mixture. From the figures, it can be concluded that liquid flow rates do not differ as much from the ideal state as compared to the vapor phase. This might be due to the inadequacy of the Redlich-Kwong equation of state to predict the liquid phase properties accurately. On the other hand, the vapor flow rates predicted based on the non-ideal equation are greater than the ideal vapor flow rates.

This is because the real residual enthalpy is lower than the ideal vapor enthalpy. Plotted in Figure 4.4 are the vapor molar enthalpies (ideal and residual) for each tray of the column. From Figure 4.4, it is shown that the non-ideal vapor enthalpy is lower compared to the ideal enthalpy. When one mol of liquid is condensed, the heat released from the condensation remains the same. However, due to the smaller vapor enthalpy, the heat required for vaporization is smaller. Therefore, for every unit of heat available, more than one mole of vapor is produced. Consequently, the vapor flow rates are higher.
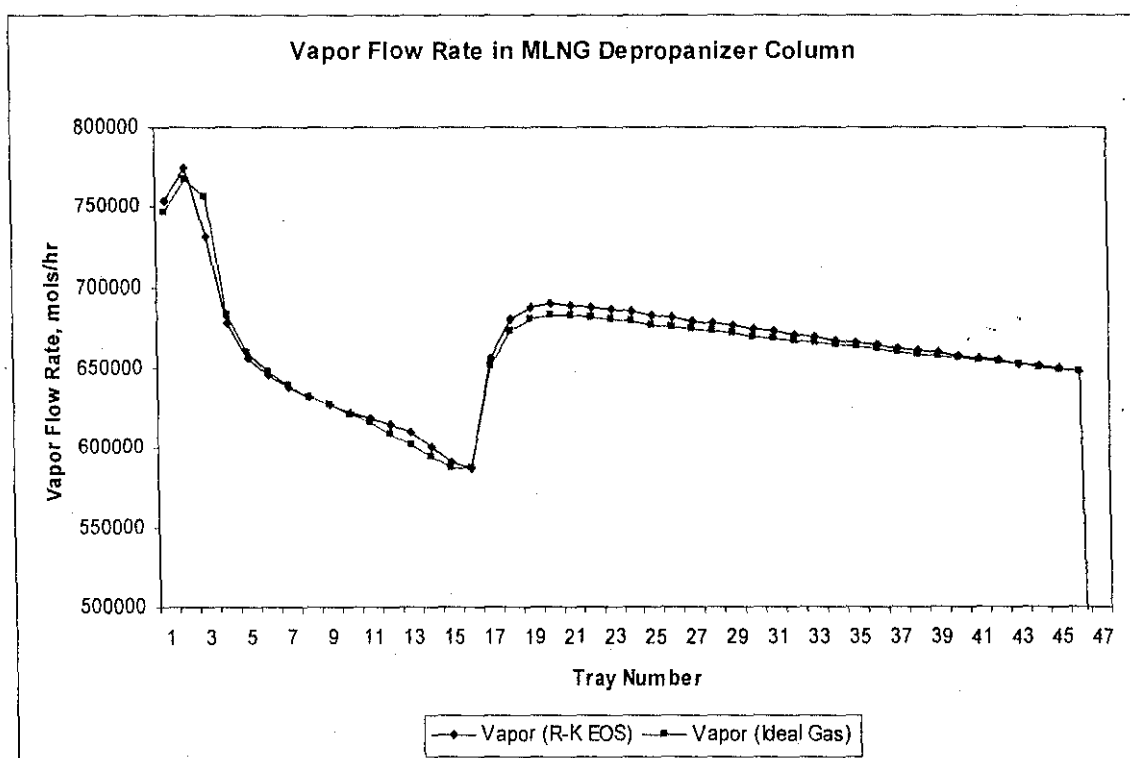

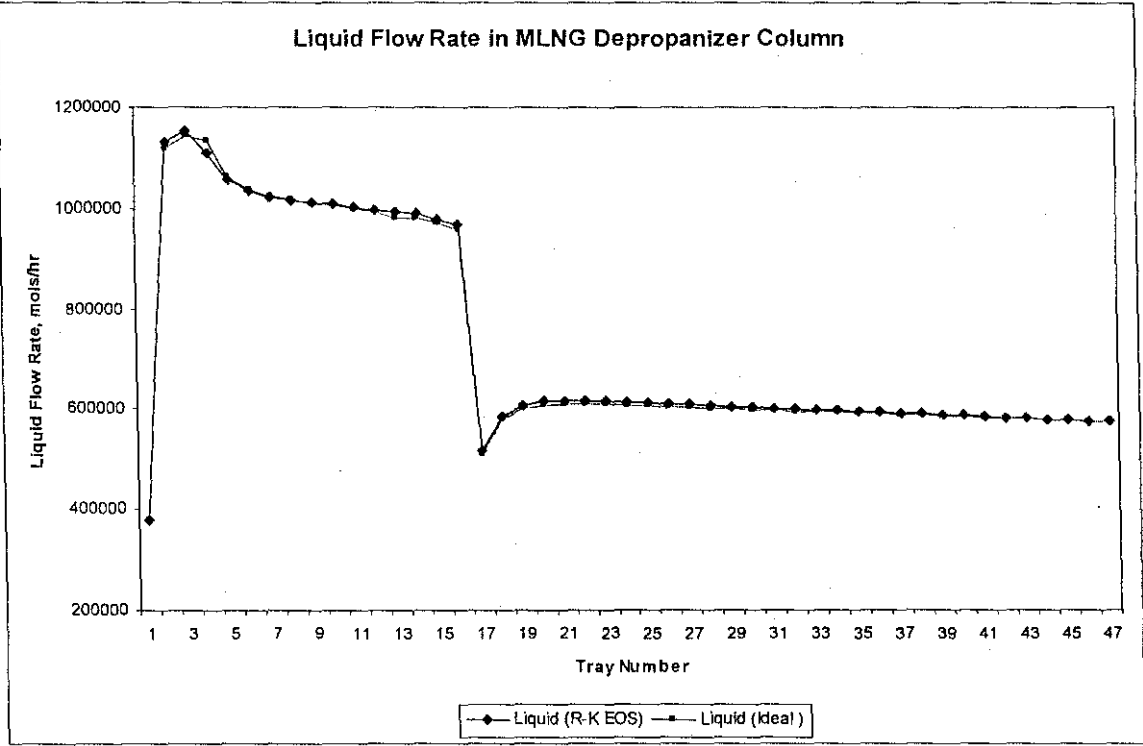Figure 4.2 Comparison of vapor flow rates for real and ideal mixture

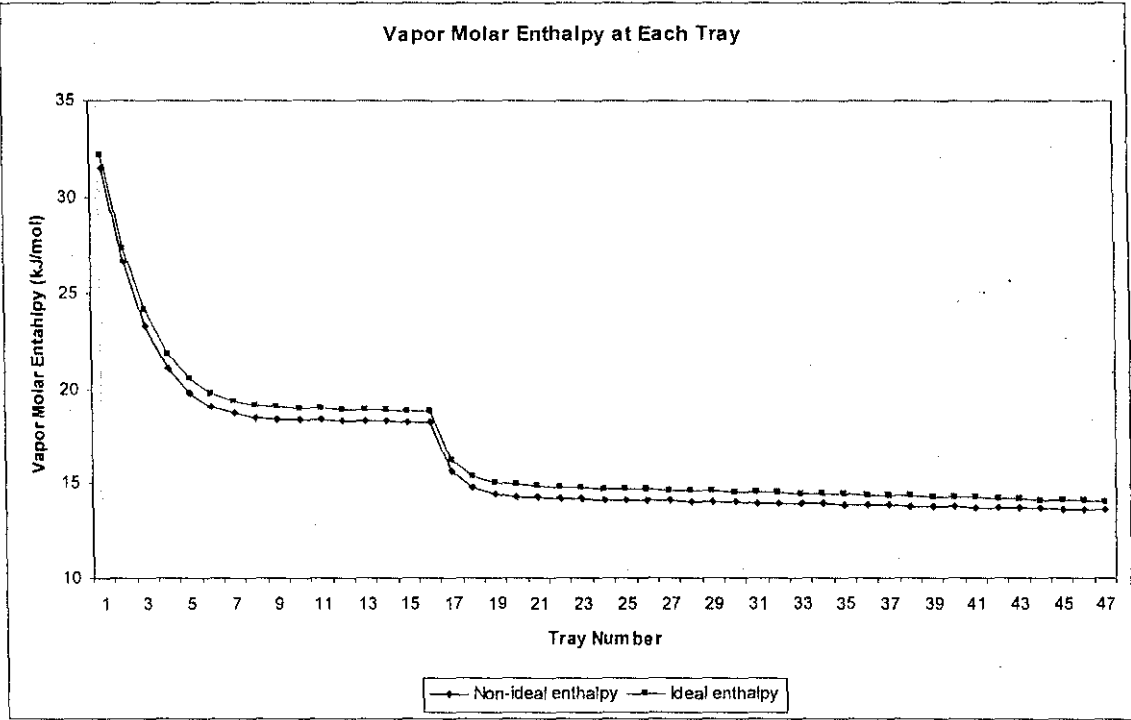Figure 4.3 Comparison of liquid flow rates for real and ideal mixture

Figure 4.4 Vapor molar enthalpy at each tray for MLNG depropanizer column

32

4.1.2 Composition Profile

In the depropanizer column, propane is the most desired product and is separated from the other heavier components. Thus, propane is the light key (LK), removed as top product. Iso-butane, on the other hand, is the heavy key (HK). The other heavier components, n-butane, iso-pentane, n-pentane and n-hexane are heavy-non-key (HNK). From Figure 4.5 and Figure 4.6, the propane composition increases as it goes up the column whereas all the other HK and HNK components decrease in their compositions.

Figure 4.7 shows the propane liquid composition profile. The rectifying stages above the feed tray purify the propane (LK) component by contacting the upward flowing vapor with successively richer liquid reflux. Stripping stages below the feed tray, however, increase the LK recovery because the vapor is relatively less concentrated in the LK component and strips the light component out of the liquid. Thus, the propane composition increases from the stripping section to rectifying section.
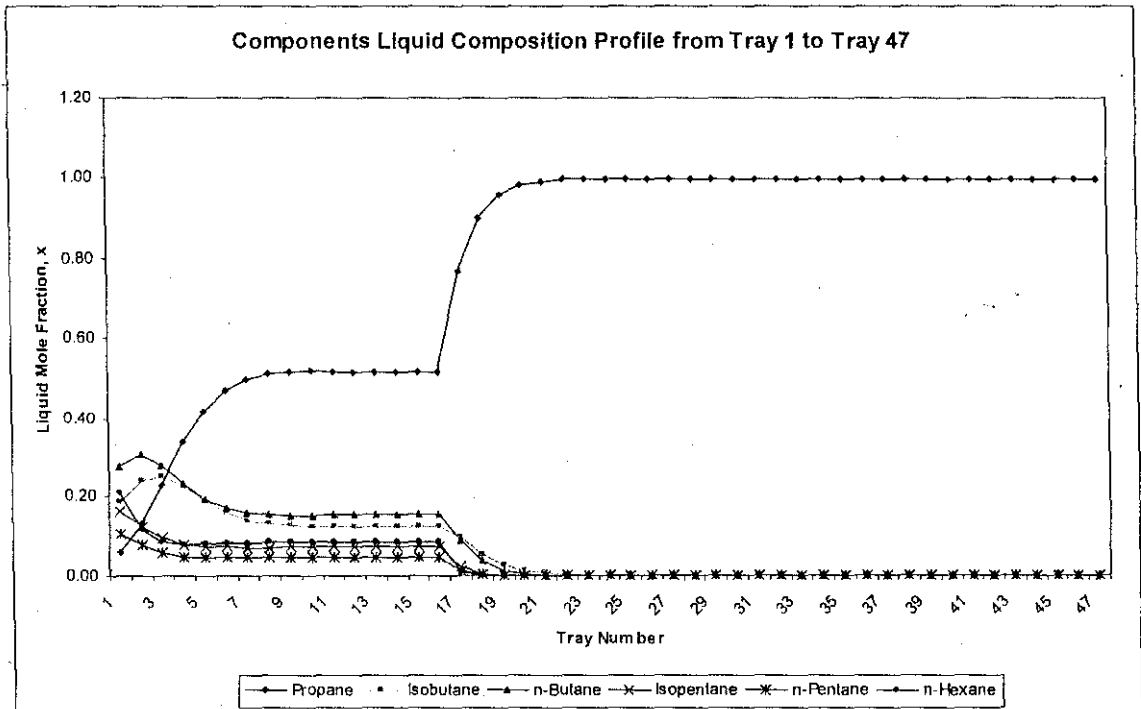

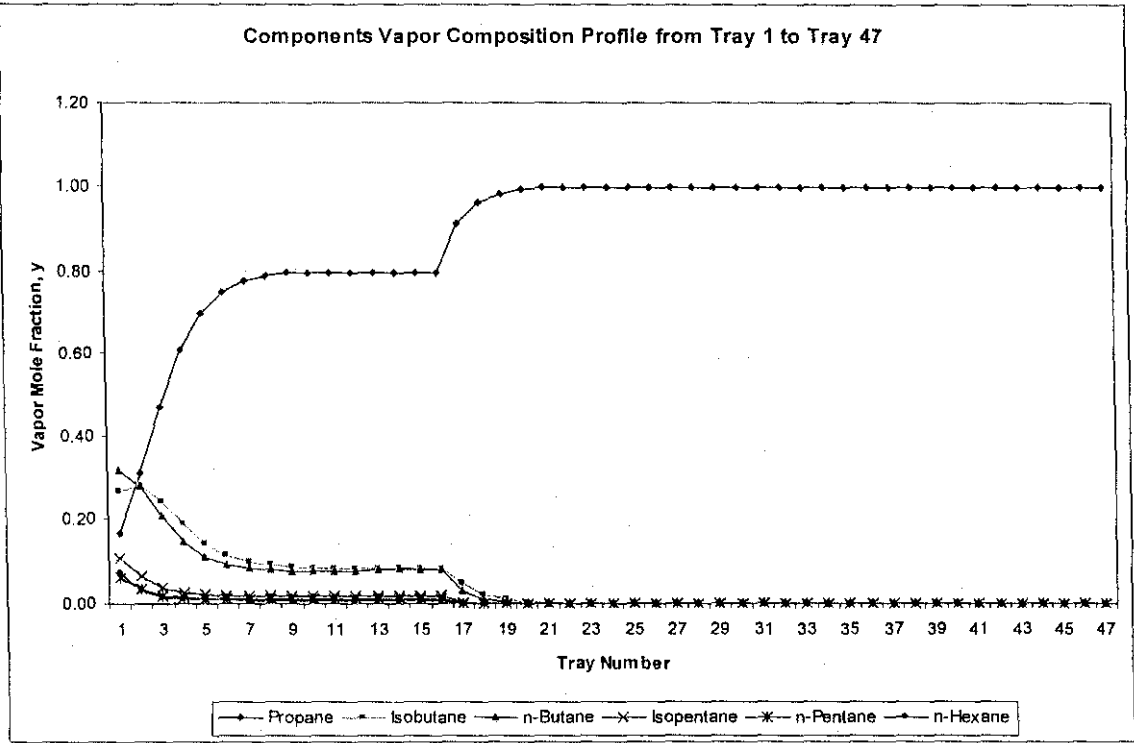Figure 4.5 Liquid composition profiles for MLNG depropanizer column

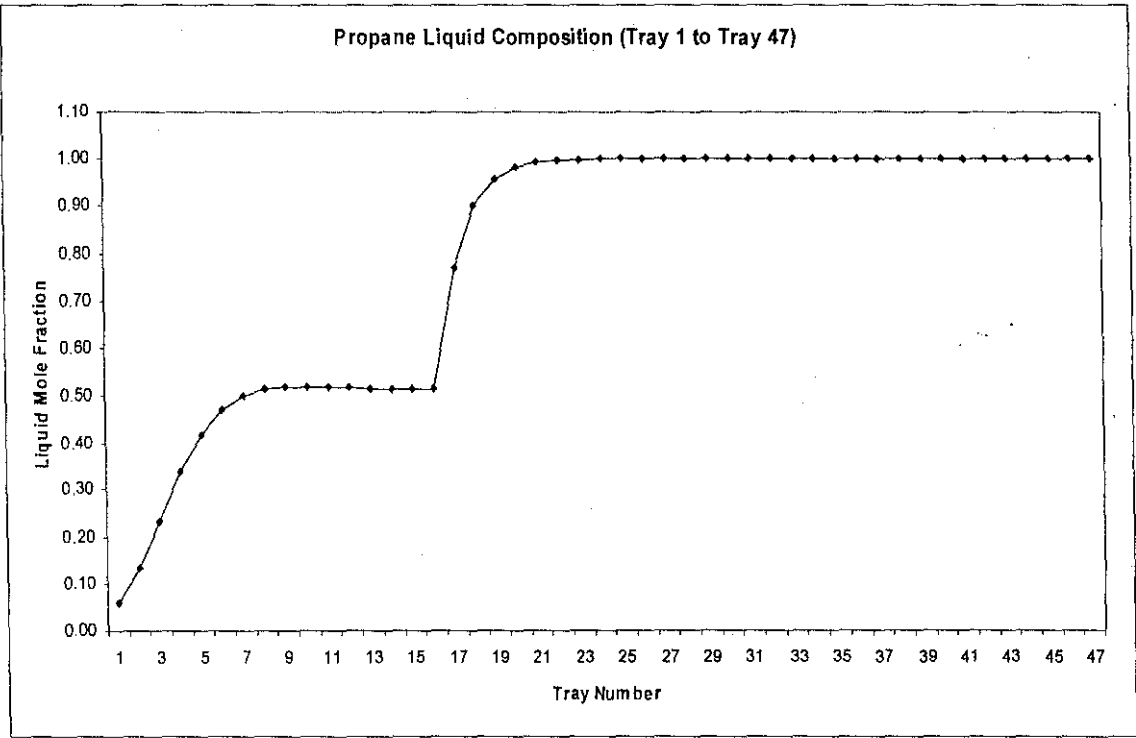Figure 4.6 Vapor composition profiles for MLNG depropanizer column

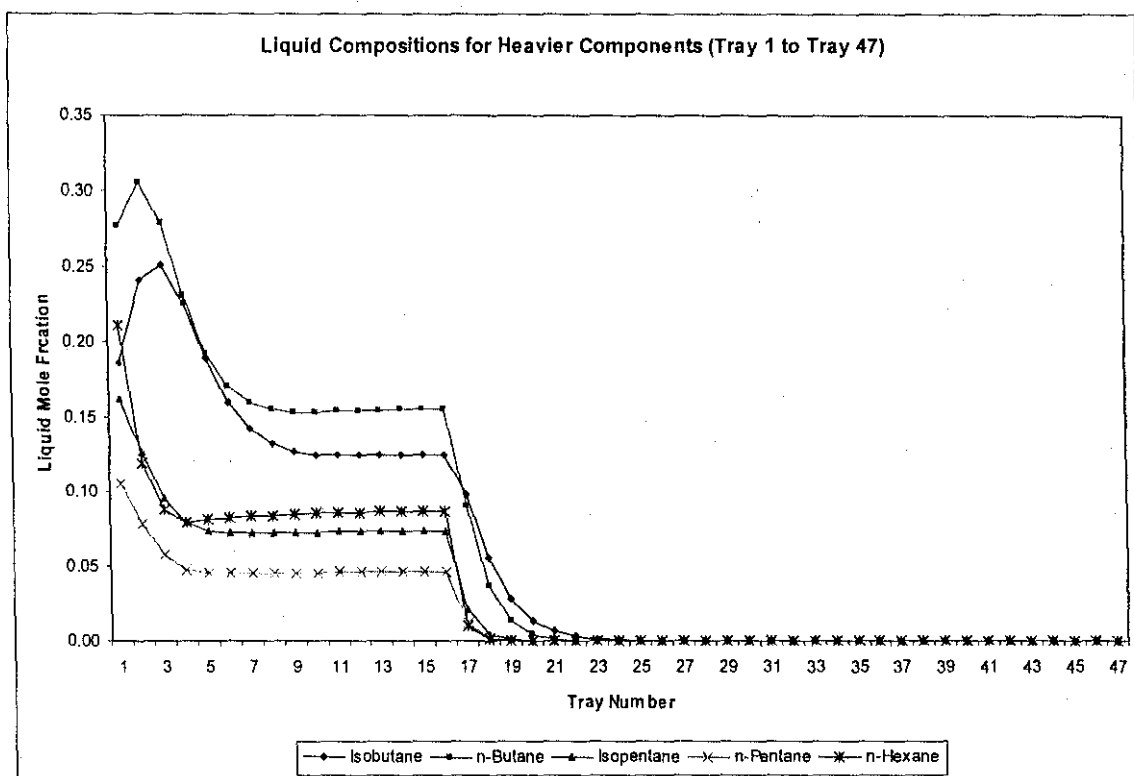Figure 4.7 Propane liquid compositions for MLNG depropanizer column

Figure 4.8 Liquid compositions of heavier components

From Figure 4.8, it is observed that butane (HK) concentration increases from tray 1 to tray 2. In the reboiler, there is very little propane (LK) and the distillation is between the heavy key and heavy-non-key. Iso-butane (HK) is the most volatile component among the heavier components distilling at the reboiler. At stage 2, iso-pentane, n-pentane and n-hexane (HNK) concentration plateaus. Thus, distillation is between light key and heavy key. At this point, the butane is less volatile and the concentration decreases. This results in maxima in the HK concentration, which peaks at tray 2.

Generally, the composition of the heavier components increases in the stripping section. The stripping section increases the purity of the heavy components. From the discussion above, the key component can have maxima. The heavy-non-keys do not distribute and appear only in the bottoms. The vapor composition profiles of propane and heavier components follow similar trend and are attached in Appendix C.

4.1.3 Temperature Profile

The temperatures of feed, condenser and reboiler, which were obtained from the average plant operational data, served as inputs of depropanizer column model. The model, with assumption of linear variation of temperature, was initialized to determine temperature at each tray. The initial assumed temperature was then corrected via bubble-point calculation and theta convergence method. Both the linear temperature variables and the converged temperature profile are shown in Figure 4.9. The temperature profile decreases steadily, stage to stage, from the reboiler to the condenser.

At the reboiler, the heavier components are being vaporized. Therefore, the temperature at the bottom section of the column is higher than the top section. From Figure 4.9, the converged temperature profile is nonlinear and exhibit two exponential curves connected at the feed tray. Because of the K values, the bubble-point and dew point equations are generally highly nonlinear in temperature.
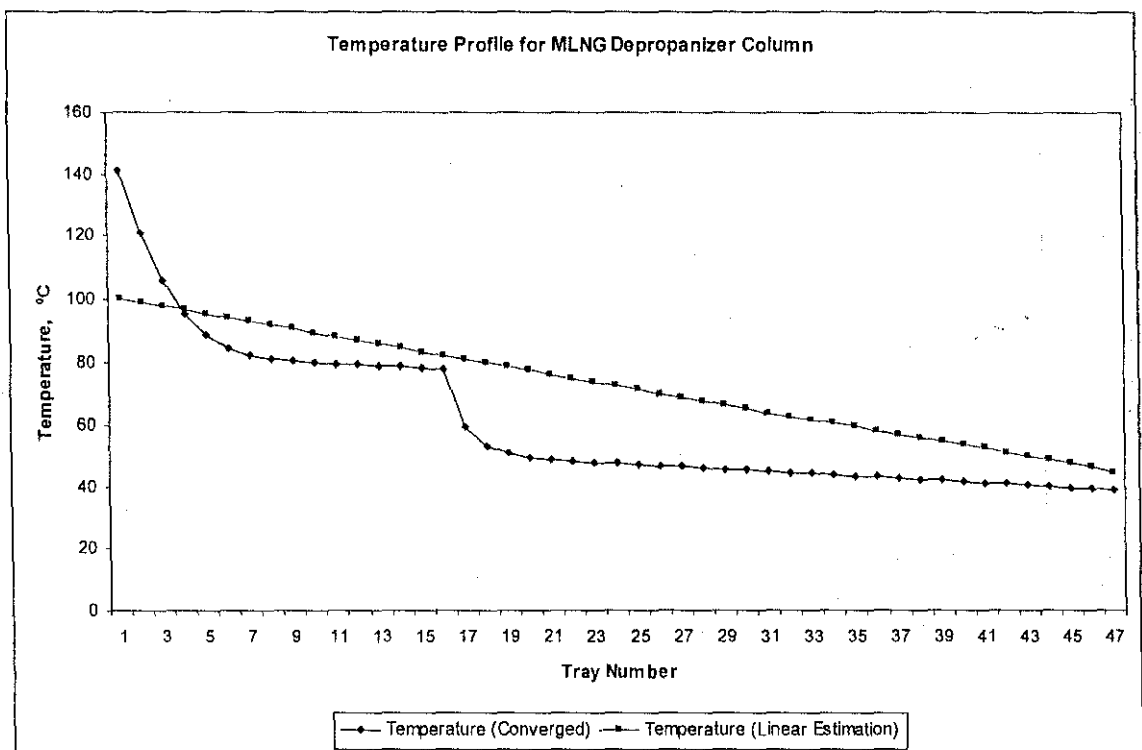

Figure 4.9 Temperature profile for MLNG depropanizer column

36

It is observed from Figure 4.9 that there is only little change in the temperature from tray 9 to tray 15 (stripping section) and from tray 19 to 46 (rectifying section). This may be due to improper feed location.

In a multi-component system, the optimum feed location depends on the light and heavy components in the system and the desired concentrations in the products.

The function of the MLNG depropanizer column is to strip as much propane as possible from stripping section. Hence, a large number of stripping trays is required whereas a small number of rectifying trays is adequate. (Khoury, 2000, p. 231) Thus, there is possibility that the rectifying section in the column is overtrayed because there are more trays in the rectifying section compared to the stripping section. Feed tray location should then be placed on a tray in the upper part of the column.

4.2 "WHAT-IF" ANALYSIS

After the depropanizer model was successfully built, the model is analyzed by varying the feed flow rate and reflux ratio. The purpose of this analysis is to test the model consistency and feasibility. "What If" analysis is carried out by varying the parameter under study, while all other parameters are held constant.

Due to the feed quality of 92.91% liquid, variations of feed flow rate do not give significant impact to the separation parameters in rectifying section (tray 17 to tray 47). Thus, only changes in the stripping section are analyzed.

4.2.1 Variation of Feed Flow Rate

The depropanizer column model was built based on a feed rate of 626.4 tons/day, which is the average value of MLNG operational data in August 2003. To carry out the

analysis, the feed flow rate was varied ±5% and ±10%. The profiles of flow rates, and compositions as well as temperature were analyzed.

As shown in Figure 4.10, liquid flow rate at stripping section of the column increases when the feed flow rate increases. However, the liquid flow at the rectifying section is affected only marginally by the feed flow rate due to the feed quality. The feed is near bubble-point and is almost saturated liquid. Thus, there will be more liquid at stripping section when feed flow rate is increased. More liquid will flow down the column as feed enters the column. This trend can be justified by internal mass balance of the column.

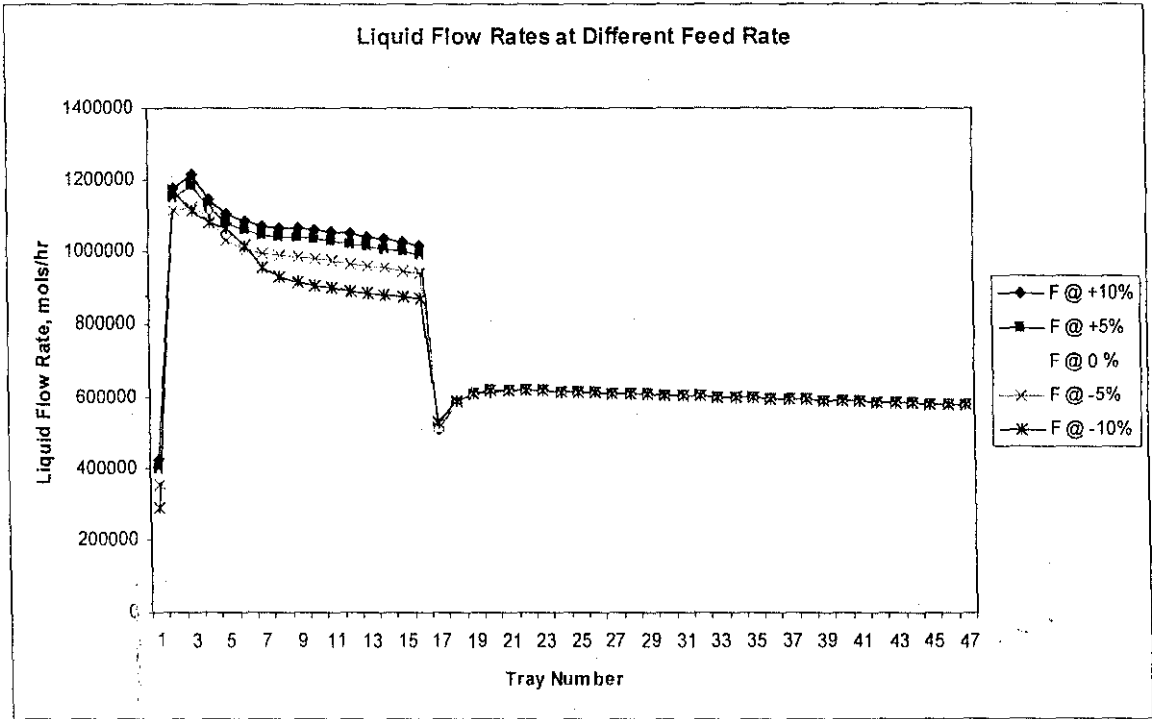Figure 4.10 Liquid flow profiles at different feed flow rates

Figure 4.11, on the other hand, shows that the vapor flow rates at stripping section decreases when feed flow rate increases. As feed flow rate increases, there are greater amount of heavier components in the stripping section of depropanizer column. The latent heat of the component increases with a greater amount of heavier components.

With the constant heat duty of reboiler, the vapor generated by the reboiler will be less due to greater latent heat of the liquid at stripping section.
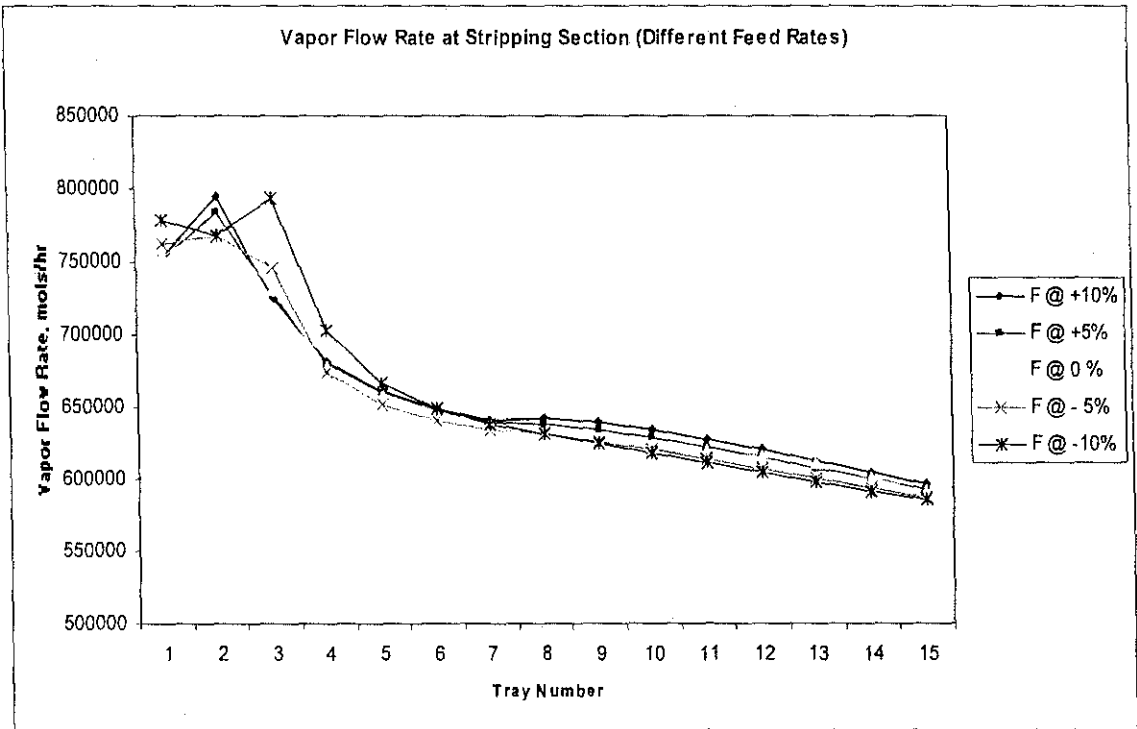

Figure 4.11 Vapor flow profiles at different feed flow rates

Similar to the liquid flow profile, the vapor flow rates at the rectifying section are not affected much by the different feed flow rate. Therefore, only the stripping section vapor flow profile is shown in Figure 4.11.

A change in feed flow rate does not give any significant change in temperature profile at rectifying section. At stripping section, the temperature decreases as the feed flow rate increases, as shown in Figure 4.12. As feed flow rate increases, the amount of propane, which is the light key, increases and this lead to increment of propane composition in stripping section. Propane has relatively low boiling point. So, even at lower operating temperature of column, the propane can be stripped off from the heavier components to rectifying section. Hence, the temperature decreases when feed flow rate increases.
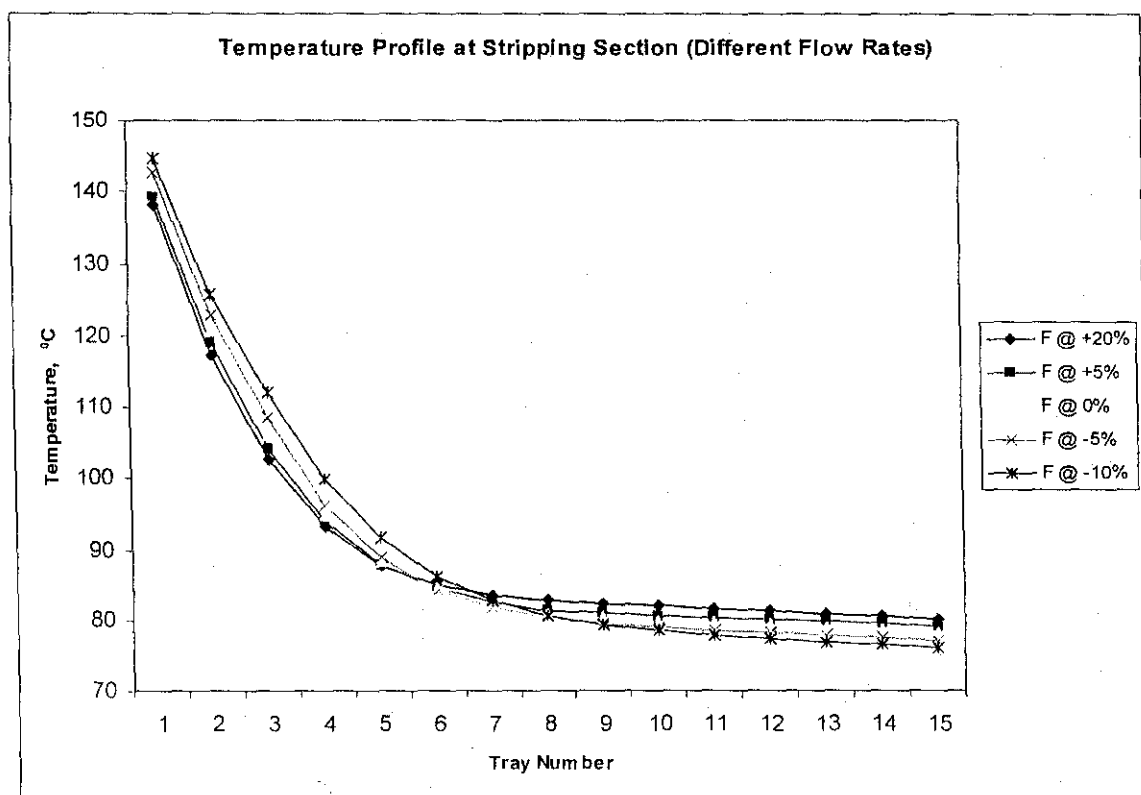
Figure 4.12 Temperature profile at different feed flow rates

The effect of feed flow rate on the propane and butane composition profiles are shown in Figure 4.13 and Figure 4.14, respectively.

Figure 4.13(a) shows the change of propane liquid composition when feed flow rate is varied. At the rectifying section, both the liquid and vapor composition profile is almost constant at different feed flow rates.

It is observed that from reboiler to tray 6, propane liquid composition increases as feed flow rate increases. This is due the increment of propane amount in the stripping section when feed flow rate increases. Since the reboiler duty remains constant, more propane exits at bottom. However, from tray 8 up to feed tray, the propane composition decreases with increasing feed flow rate as shown in Figure 4.13(b). Propane vapor composition profile is shown in Figure 4.13(c).
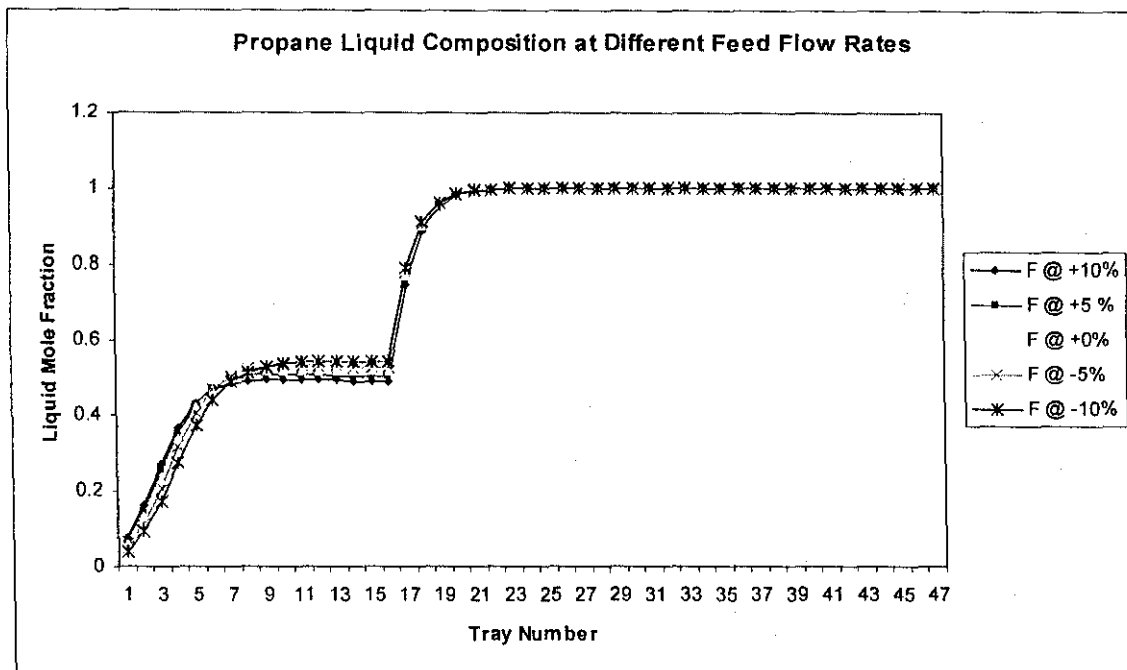
Figure 4.13(a) Propane liquid composition profile at different feed flow rates
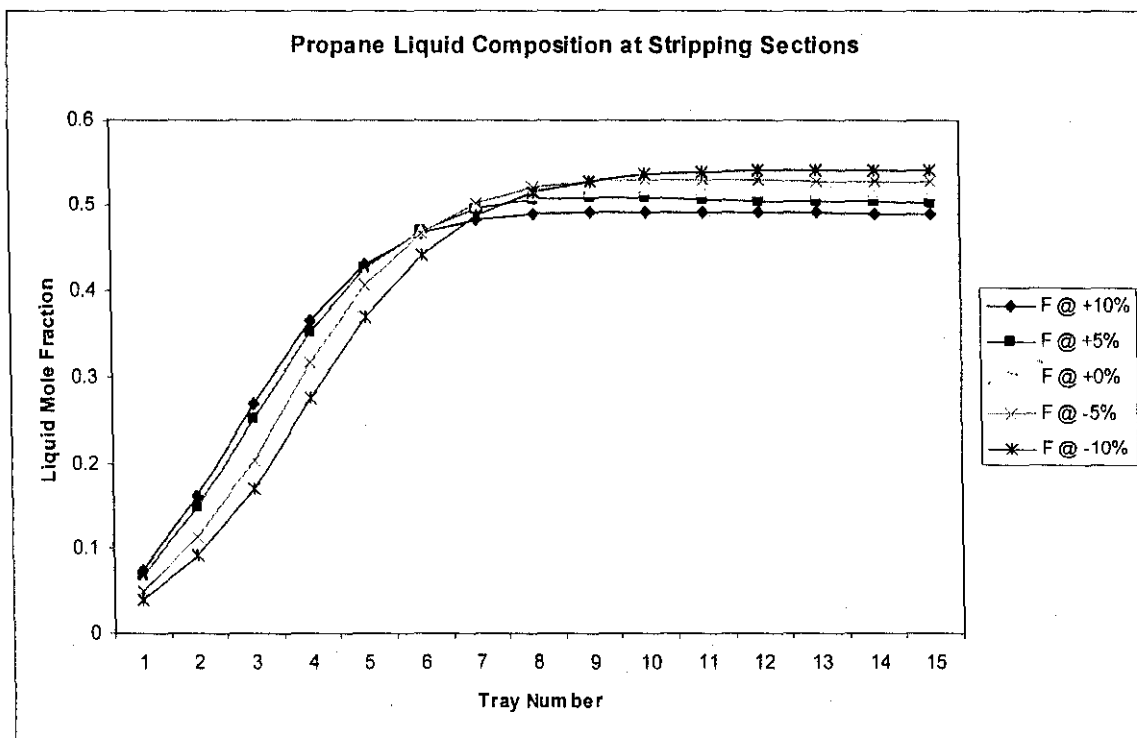

Figure 4.13(b) Propane liquid composition profile at different feed rate (Stripping section)

Propane Vapor Compostiion at Stripping Section
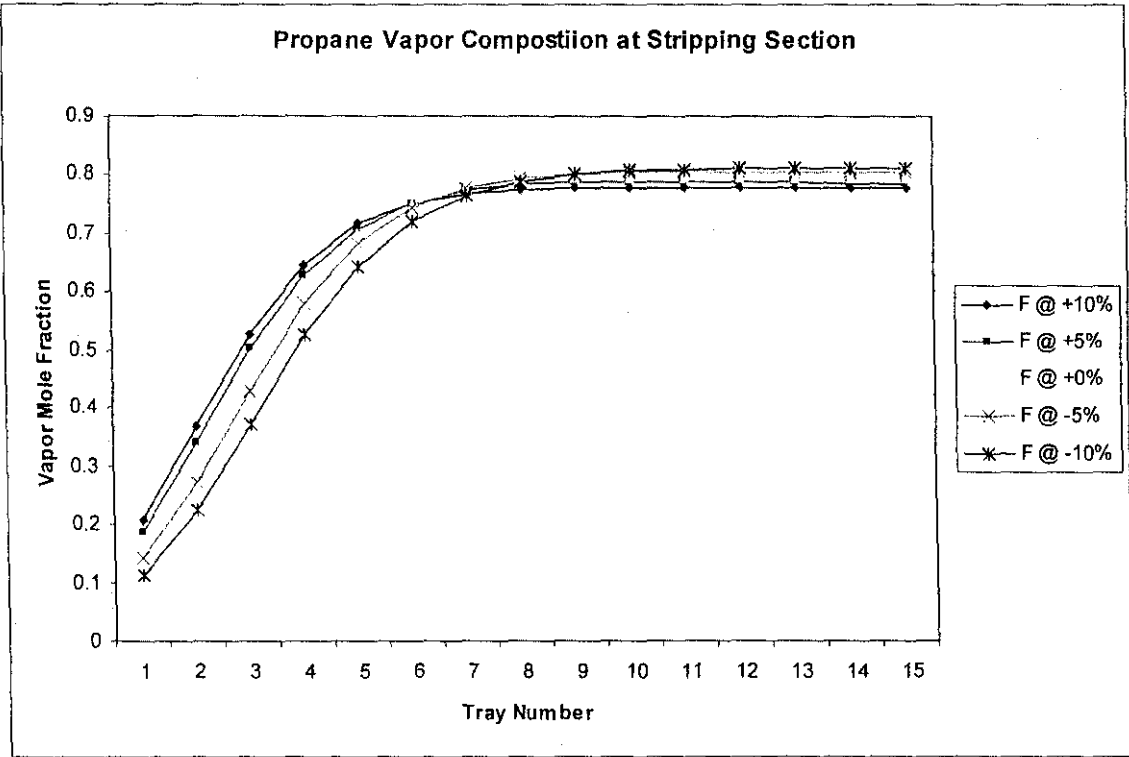
Figure 4.13 (c) Propane vapor composition profile at different feed rates (Stripping section)

For other components that are heavier than propane, the liquid and vapor compositions at stripping section decrease from tray 1 to tray 7 as feed flow rate increases. From the principle of mole fraction summation, all mole fraction summation equals to one. Propane composition increases as feed rate increases. Thus, the compositions of heavier components in the stripping section decrease as feed flow rate increases. On the other hand, from tray 8 up to feed tray, the heavier components liquid and vapor compositions are greater at higher feed flow rate. This may be due to improper feed location as discussed in previous section.

Figures 4.14(a) and 4.14(b) shows the liquid and vapor composition of n-butane, which is one of the heavier components. The composition profiles for other heavier components are presented in Appendix D.

Figure 4.14 (a) n-Butane liquid composition profile at different feed flow rate (Stripping section)

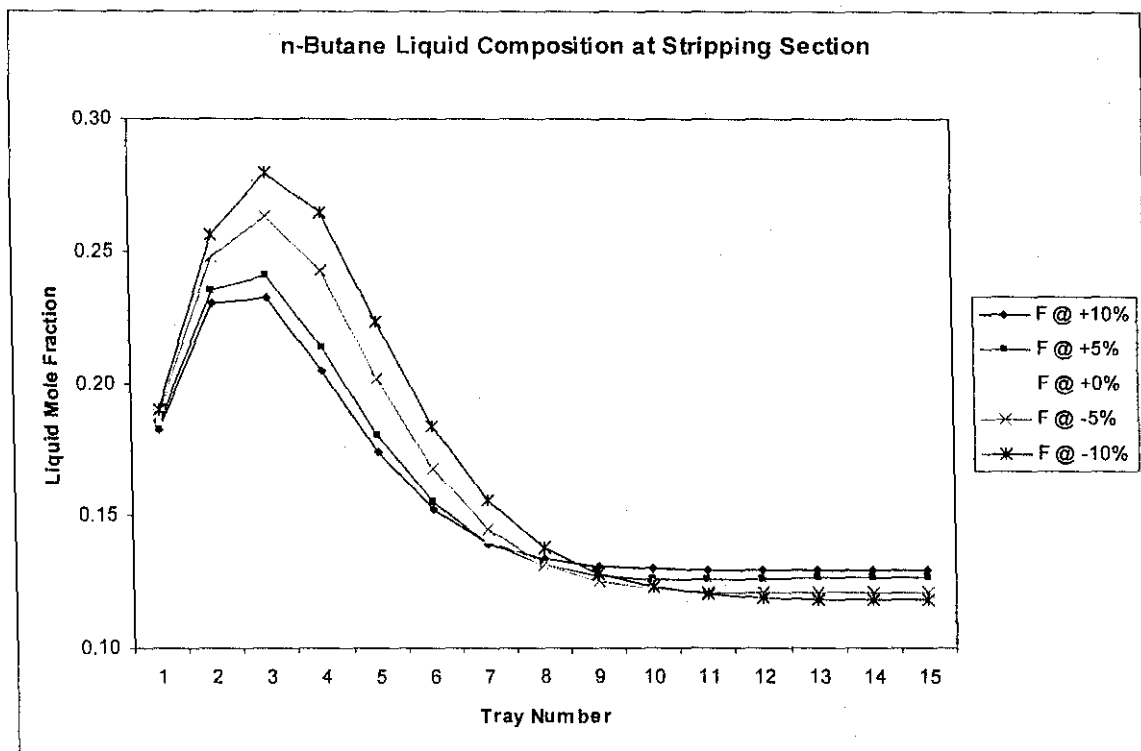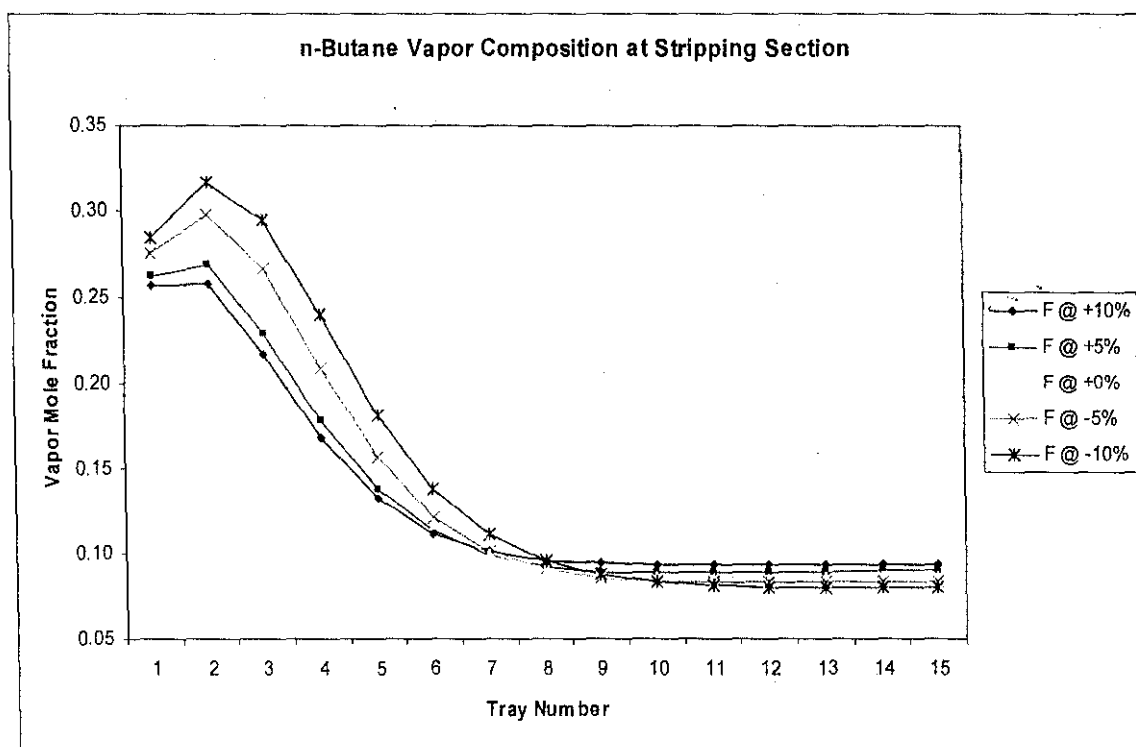Figure 4.14 (b) n-Butane vapor composition profiles at different feed flow rate (Stripping section)

43

4.2.2 Variation of Reflux Ratio

The reflux ratio adapted in this column model is 8, which was based on MLNG operational data August 2003. To carry out "What If" analysis, the reflux ratio was varied with the values of 6 and 9. The reflux ratio is varied while the feed flow rate and distillate are held constant.

The effect of reflux ratio on the liquid and vapor flow profiles are analyzed in Figure 4.15 and Figure 4.16, respectively. It can be concluded that the liquid and vapor flow rates are higher at higher reflux ratio. Reflux ratio (RR) is defined as the ratio of the reflux (R) to the distillate (D) where reflux is the liquid that is recycled back to the top of the main column.

$$RR = \frac{R}{D}$$
(Eq.40)

From (Eq.40), when the distillate flow is constant, the reflux increases as reflux ratio increases. With an increase in reflux, more liquid is recycled back into the column, resulting in an increased liquid flow in the column at all trays. The liquid flow is increased by approximately a value equivalent to the amount of increment in reflux flow. This is shown in Figure 4.15 where the increment in liquid flow is almost constant throughout the column.

In order to maintain 98% of propane recovery at the distillate, more vapors must be generated by the reboiler as the liquid flow increases. Therefore, the vapor flow in the column also increases with increasing reflux ratio, as shown in Figure 4.16.
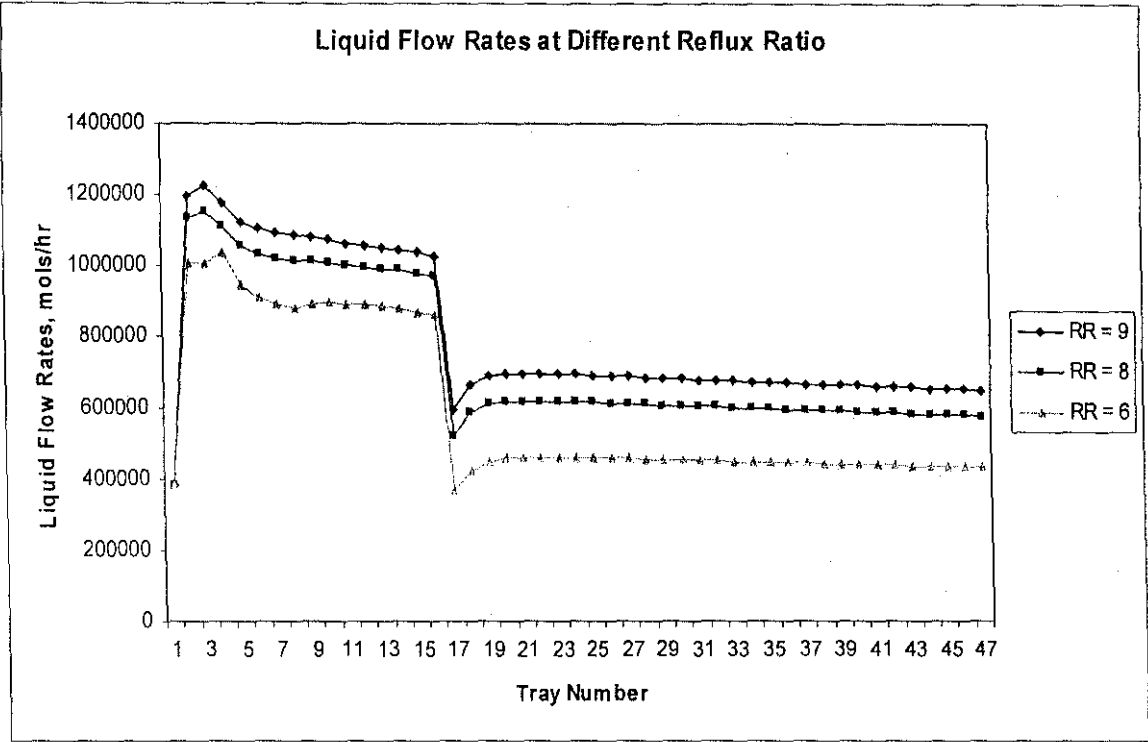
44

Figure 4.15 Liquid flow profiles at different reflux ratio
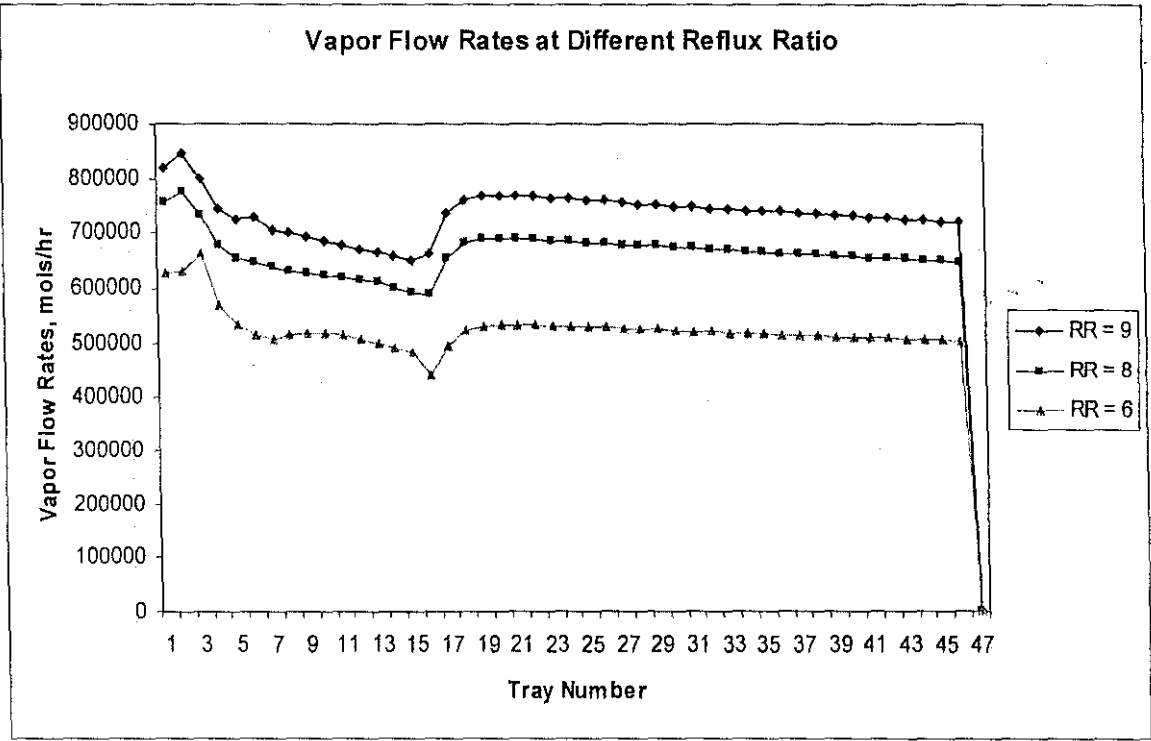
Figure 4.16 Vapor flow profile at different reflux ratio

45
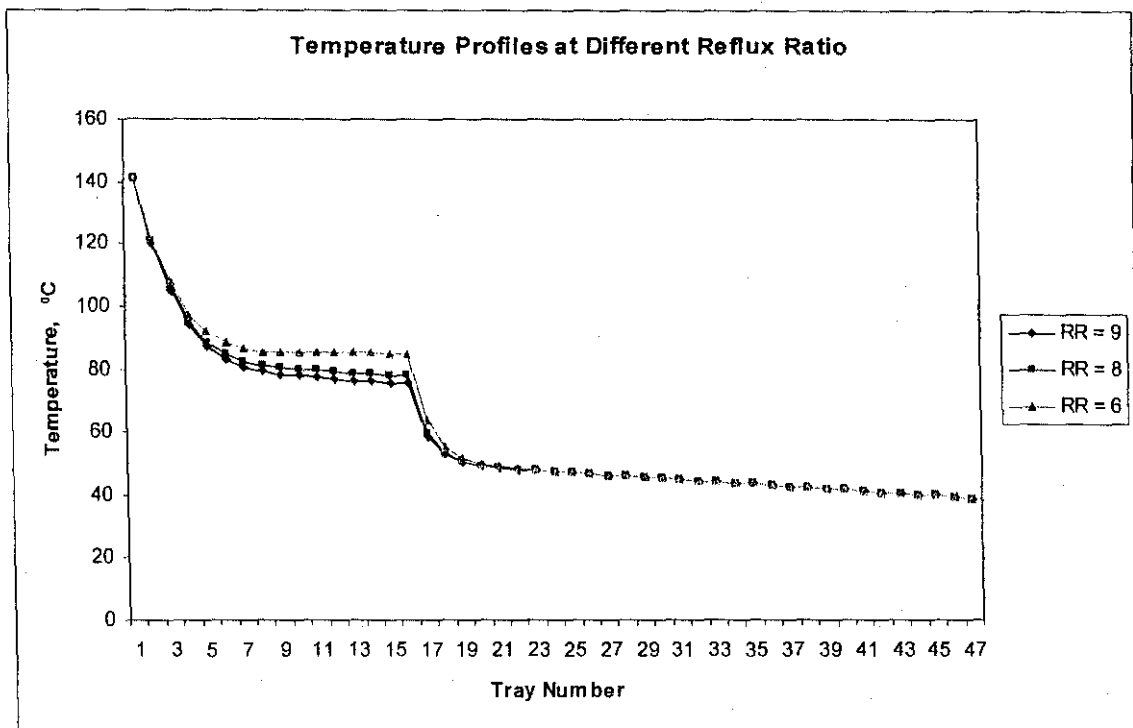
Figure 4.17 Temperature profile at different reflux ratio

Temperature profile is shown in Figure 4.17. At stripping section, temperature decreases with increasing reflux ratio. This is due to two reasons. Firstly, reflux flow itself cools the column. One of the purposes of returning reflux into the column is to cool down the column. Thus, as reflux ratio increases, more cooling is achieved. Secondly, the column operating temperature is lower because the reflux is rich in light components, which have relatively lower boiling point. Since the product compositions do not vary greatly at constant product rate, the product temperatures do not vary much with reflux ratio.

Reflux and distillate streams have the same composition. Since the distillate is rich in light components, reflux also is rich in light components. Hence, at higher reflux ratio, propane (light component) composition is greater. Overhead is richer in light component. On the other hand, the heavier components compositions decrease when reflux ratio increases. The propane and n-butane composition profiles are presented in Figures 4.18 and 4.19, respectively. Only n-butane, one of the heavier components, compositions profiles are shown in Figures 4.19(a) and (b). The other heavier components profiles are attached in Appendix D.

46

Figure 4.18 (a) Propane liquid composition at different reflux ratio
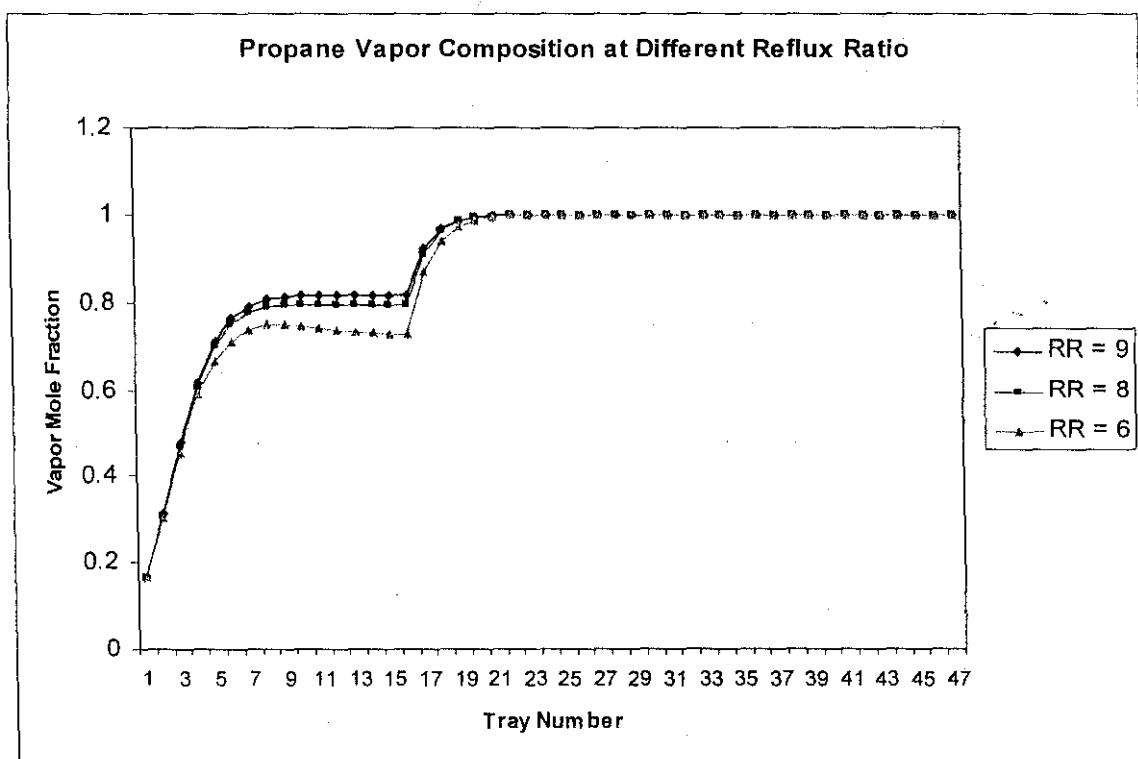
Figure 4.18 (b) Propane vapor composition at different reflux ratio
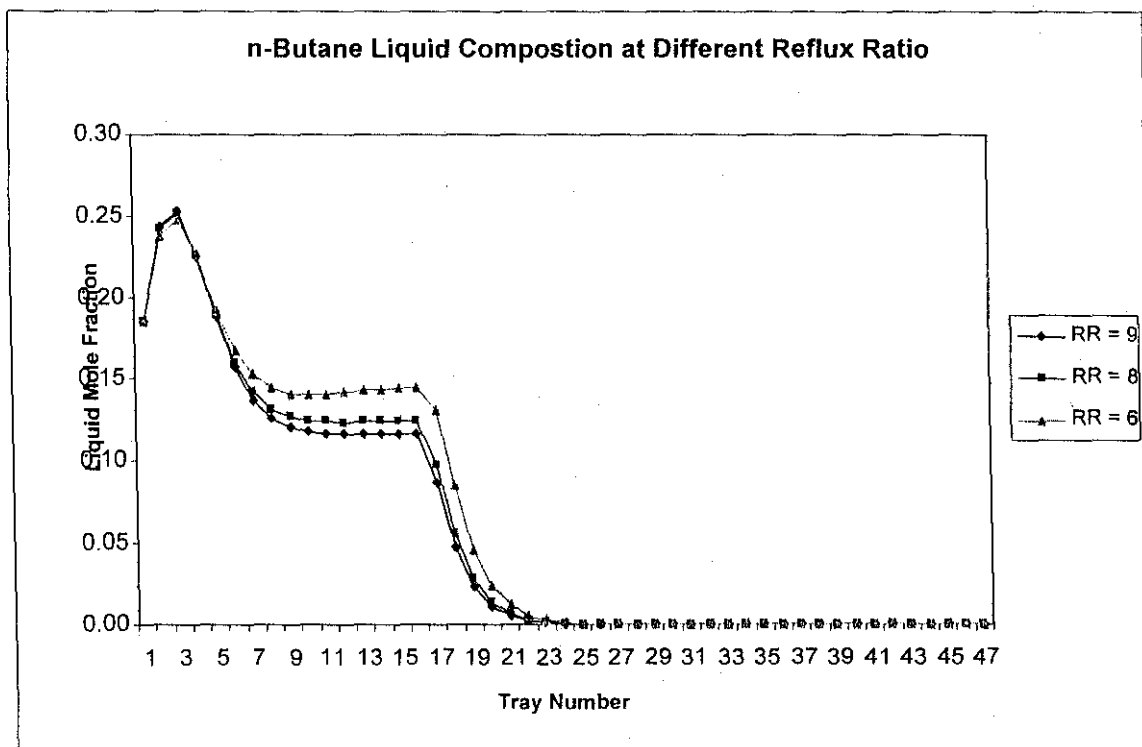
Figure 4.19 (a) n-Butane liquid composition at different reflux ratio
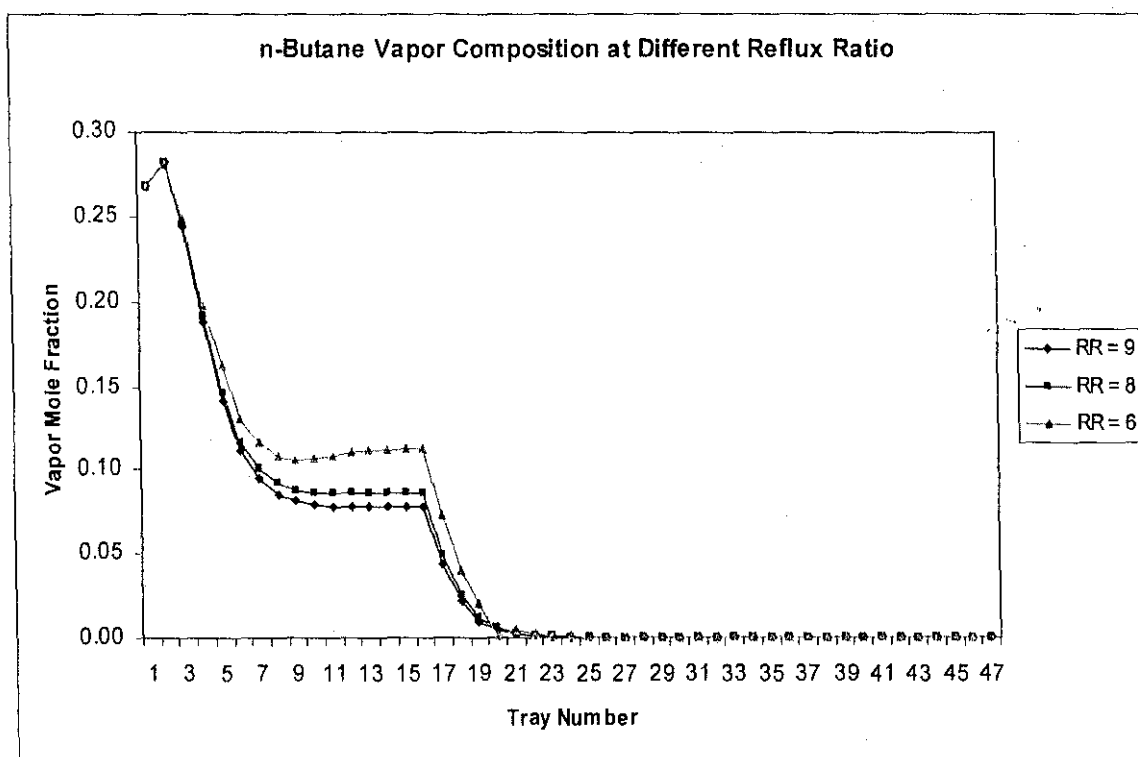
Figure 4.19 (b) n-Butane vapor composition at different reflux ratio
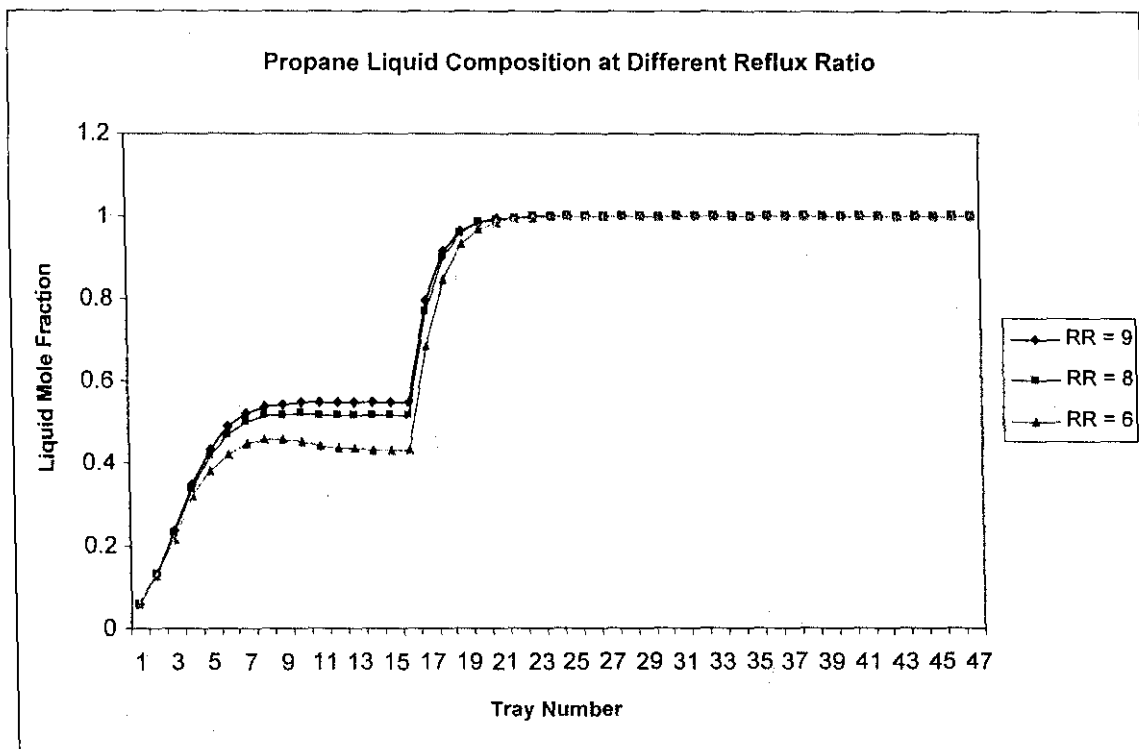
4.3   ASSUMPTION ANALYSIS

The assumptions made in the MLNG depropanizer column model include:

1. 100% tray efficiency
2. Narrow boiling feed mixture

4.3.1   100 % Tray efficiency

The model was developed with the assumption that the vapor and liquid leaving a tray are in equilibrium. In reality, due to mass transfer limitations, the vapor and liquid streams will not be in equilibrium. Tray efficiency may be much less than 100%. Therefore, it affects the separation of components on each tray.

From the created model, the top product (propane) composition reaches the desired purity at tray 29, which is far below the condenser (tray 47). The actual plant data indicates that this composition is only achieved at tray 34. If tray efficiency is incorporated into the model, a shift to the right in the composition profile is anticipated. In other words, propane would only reach purity at a much higher tray than tray 29.

Hence, the depropanizer column model can be improved by incorporating tray efficiency into the working model.

4.3.2   Narrow boiling feed mixture

Narrow-boiling point mixture is a mixture that boils over a relatively narrow temperature range, meaning that the bubble point and dew point are close. In narrow-boiling mixtures, the calculation of stage temperature is more sensitive to the liquid phase composition. The purpose of this assumption is to ease the process of modeling. Only with this assumption, bubble-point calculation method can be used for temperature convergence calculations.

Wankat (1988, p. 251) stated that distillation problems converge best if a narrow-boiling feed calculation is done instead of a wide-boiling feed calculation. Furthermore, the feed mixture to the depropanizer column contains hydrocarbons of $C_3 - C_8$ range, which have relatively close boiling points and also are chemically similar.

4.4 PROBLEMS ENCOUNTERED

4.4.1 Computation of Residual Enthalpies

The computation of residual enthalpies using Redlich-Kwong equation of state results in a very complex process of modeling due to the equations employed. In general, at supercritical temperatures, where only one phase can exist, one real root and a complex conjugate pair of roots are obtained from (Eq.37). Below critical temperatures, where vapor and/or liquid phases can exist, three real roots are obtained.

$$Z^3 - Z^2 + (A - B - B^2)Z - AB = 0 \qquad \text{(Eq. 39)}$$

When the depropanizer column model was first developed, one real root and a pair of complex roots were obtained for stage 2 to stage 16. This implied that these stages exist at supercritical temperature and only one phase can exist, which is not true. Therefore, the problem was investigated. After much effort, it was identified that inaccuracy in the first initial tear values for stage temperatures led to the error. Therefore, the constants for the EOS equations were calculated only after the temperature convergence loop.

4.4.2 Accuracy of Redlich-Kwong EOS in Liquid Phase Properties

Although the thermodynamic properties of liquid can be calculated by means of cubic equations of state, the results are often not of high accuracy. (Smith, et. al., 1996, p. 94) As a result, the liquid phase results obtained were not very accurate.

Several equation of state had been developed with improved accuracy such as Soave and Peng Robinson equations. They are widely used for hydrocarbons over broad ranges of temperature and pressure. Both the Soave and Peng Robinson equations are accurate enough for calculating enthalpy departures for both vapor and liquid phase. Thus, for improved accuracy, the Peng Robinson equation may be adapted for future work.

Apart from applying the Soave-Redlich-Kwong and Peng Robinson EOS, more accurate methods are available. According to Winnick (1997, p. 358), a different approach to nonideality is taken for liquids. A correction factor is added to the properties of the ideal solution. This correction factor is the liquid activity coefficient, γ_i.

For liquid phase, instead of residual properties, the extensive properties of a real solution are related to the ideal properties through terms called excess function. Therefore, the enthalpy calculation of the liquid phase will be more accurate if the excess enthalpies on mixing are calculated. The excess enthalpy, h^E, is defined as the difference between the real and ideal solution enthalpies at the same T, P and x, given by the equation below.

$$h^E = h_M - h_M' = \sum x_i H_i - \sum x_i h_i \qquad \text{(Eq.41)}$$

where $\dfrac{\partial(g^E/T)}{\partial T} = -\dfrac{h^E}{T^2}$

g^E = excess Gibbs energy

$= RT \sum x_i \ln \gamma_i$

Activity coefficients can be estimated from empirical correlations. However, only correlation suitable for hydrocarbon mixtures should be used. The computation of excess enthalpy and related parameters are detailed out by Winnick. (1997, p. 364) Attempts had been made to incorporate the excess enthalpy properties for the liquid phase. However, due to the complexity of the activity coefficient equations and time constraint, the modification was not carried out successfully.

CHAPTER 5

CONCLUSIONS AND RECOMMENDATIONS

5.1 CONCLUSION

The objective of this project has been achieved successfully. A functional model of a depropanizer column was successfully built using plate-to plate material and energy balances calculations, incorporating the non-ideal gas Redlich-Kwong equation of state. The model developed successfully eliminates the assumption of constant molar overflow as well as ideal gas assumption. The assumptions that were employed in building this model include:

1. 100% tray efficiency
2. Narrow-boiling feed mixture

The results from the "What-If" analysis serve as a useful strategy for off-line optimization. The optimum operating conditions such as feed input and reflux ratio can be predicted by the model. These optimum operating conditions can then be used to optimize the depropanizer column in order to maximize profit.

In conclusion, this project has formed the groundwork for the future optimization study of MLNG depropanizer column.

5.2   RECOMMENDATIONS

Even though the project has achieved the objectives set, there is scope for future work in order to further improve the depropanizer column model. The following recommendations are made to further enhance the model developed:

1. It is recommended that tray efficiency parameter should be incorporated into the depropanizer column model. This will give a better prediction on depropanizer column operation conditions.

2. In order to improve the accuracy of the flow and composition profiles predicted, it is recommended to compute the non-ideal liquid molar enthalpies using excess enthalpy calculation.

3. It is also recommended to compute non-ideal enthalpies using equation of state with greater accuracy such as Peng-Robinson.

4. It is recommended to include other operating conditions such as feed quality, column temperature and product rates in the "What If" analysis to further optimize the depropanizer column.

5. It is recommended to obtain more data input on MLNG depropanizer column's operational parameters in order to obtain better estimation of first tear variables.

6. To test the accuracy of the model, it is proposed to use HYSYS simulation to countercheck the result of the model.

REFERENCES

Doherty M.F. and Malone M.F., 2001, *Conceptual Design of Distillation Systems*, New York, McGraw Hill

Geankoplis C. J., 1995, *Transport Processes and Unit Operations*, New Jersey, Prentice Hall, p.679 - 680

Hahn B.D., 2002, *Essential MATLAB for Scientists and Engineers*, Oxford, Butterworth-Heinemann

Khoury F. M., 2000, *Predicting the Performance of Multistage Separation Processes*, New York, CRC Press

King C. J., 1980, *Separation Processes*, New York, McGraw Hill.

Kister H. Z., 1992, *Distillation Design*, New York, McGraw Hill

Najim K., 1989, *Process Modeling and Control in Chemical Engineering*, New York, Marcel Dekker Inc.

Orbey H. and Sandler S.I., 1998, *Modeling Vapor-Liquid Equilibria: Cubic Equations of State and Their Mixing Rules*, United Kingdom, Cambridge University Press.

Perry R.H and Green D.W., 1999, New York, McGraw-Hill, Perry's Chemical Engineer's Handbook CD-ROM

Ramirez W. F., 1997, *Computational Methods for Process Simulation*, Oxford, Butterworth-Heinemann

Seader J. D. and Henley E. J., 1998, *Separation Process Principles*, New York, John Wiley and Sons

Siva Subramaniam S.G., November 2003, *Modeling of the Depropanizer Column of MLNG*, Universiti Teknologi Petronas, Perak, Malaysia

Smith J.M., Van Ness H.C., Abbott M.M., 1996, *Introduction to Chemical Engineering Thermodynamics*, United States, McGraw-Hill.

Stichlmair J. G., Fair J. R., .1998, *Distillation Principles and Practices*, NewYork, Wiley-VCH

Tan Khang Meei, April 2004, Plate-to-Plate Material and Energy Balances Calculations for MLNG Depropanizer Column, Universiti Teknologi Petronas, Perak.

Tham M.T., 2000, <http://lorien.ncl.ac.uk/ming/distil/dist-trays.htm.>

UK Trade and Investment, 1 July 2003, <http://www.uktradeinvest.gov.uk/oilandgas/malaysia/profile/overview.shtml>

Wankat P. C., 1988, *Equilibrium Staged Separations*, New Jersey, Prentice Hall

APPENDICES

APPENDIX A: PSEUDO CODE FOR PROGRAM

I) Pseudo code for convergence of mass balances and temperature loop (modification of Shri Gugan Siva Subramaniam's and Tan Khang Meei's model)

1.   Get input
   - a.   Feed rate,   F
   - b.   Feed Compositions,   z
   - c.   Feed temperature,   Tf
   - d.   Estimated C_3 fraction in distillate,   xad
   - e.   Reflux ratio,   RR
   - f.   Distillate flow,   D
   - g.   Condenser temperature   T_con
   - h.   Reboiler temperature   T_reb
   - i.   Condenser pressure   P_con
   - j.   Reboiler pressure   P_reb
   - k.   Number of stages   N
   - l.   Feed stage number   Nf

2. Calculate bottoms flowrate   B
3. Calculate liquid flow in column
4. Determine liquid flow at each stage, j L_j
5. Calculate vapor flow in column in
6. Determine vapor flow at each stage V_j
7. Calculate Distillate component compositions   xid
8. Calculate Bottoms component compositions   xib
9. Determine Temperature of each stage, j   T(j)
10. Calculate Pressure for each stage, j   P(j)
11. Calculate K values for each component at each stage K_{ij}
    - For $(1 \le j \le N)$
    - a.   Invoke function files for equilibrium calculation
    - b.   Obtain $K_{ij} = fki\ (T_j, P_j)$,
    -     Where fki = fka.m, fkb.m ... fkf.m

Component Mass Balances

1. Calculate values for mass balance matrix (Eq.8) A_j, B_j, C_j and D_j
2. Build ABC matrix (NxN); I matrix (Nx1) and D matrix (Nx1)
3. Equate matrixes as ABC * I = D
4. Solve for all l_j in matrix I l_{ij}
   - Invert matrix ABC and multiply with matrix D
5. Repeat steps 1 to 5 for remaining components

Theta Convergence Method

1. Find theta that satisfies Eqn   5 ϑ
   - a.   Input necessary parameters into function files fcn1 and fcn2
   - b.   Calculate theta from output of function file until convergence
   -     Theta = theta output of fcn1 / output of fcn 2
2. Correct component flow rates $l_{ij,corr}$
3. Determine component mole fractions x_{ij}
4. Repeat calculations for all elements
5. Calculate new temperatures for all stages   T_new
   - a.   Using bubble point procedure
   - b.   Invoke function file fcnT
6. Calculate new K-values K_{ij}
7. Calculate new coefficients for ABC and D matrixes A_j, B_j, C_j, D_j
8. Calculate new values for component flow rates for all components l_{ij}
9. Perform theta convergence procedures until temperature loop converges ϑ

II) Pseudo codes for function files of mass balances (source: Shri Gugan a/l Siva Subramaniam's model)

    i. Equilibrium constant (K) model

1. Obtain input (temperature pressure) from primary programme
2. Convert temperature from degrees Celcius to Rankine
3. Convert pressure from Pascal to Psia
4. Specify values for coefficients aT1, aT2, aT6, ap1, ap2 and ap3 for each component
5. Calculate equilibrium constant K value and return to main programme

    ii. Temperature reverse calculation model

1. Obtain input from primary program
2. Convert pressure from Pascal to Psia (P)

3. Specify values for coefficients aT1, aT2, aT6, ap1, ap2 and ap3 for propane
4. Calculate value for coefficient a
5. Calculate value for coefficient c

   c = aT1

6. Calculate the root of the equilibrium K expression for propane
7. Convert the temperature from rankine to Kelvin and return to main programme

iii. Theta calculation model

Function 1

1. Obtain input from primary programme
2. Set initial value of function f1 equals to 0
3. Set values of Bxibot_calc and Dxidist_calc for each component

   Bxibot_calc(c) = component flow at reboiler

   Dxidist_calc(c) = component flow at condenser (c) / Reflux Ratio

4. Calculate value for function f1

   Calculate value for function fcn1 and return to main programme

Function 2

1. Obtain input from primary programme
2. Set initial value of function f2 equals to 0
3. Set values of Bxibot_calc and Dxidist_calc for each component

   Bxibot_calc(c) = component flow at reboiler

   Dxidist_calc(c) = component flow at condenser (c) / Reflux Ratio

4. Calculate value for function f2
5. Calculate value for function fcn2 and return to main programme

III) Pseudo code for convergence of non-ideal energy balance

1. Assign a new term for vapor and liquid flow rates from mass balance
2. Calculate empirical constants, a and b
   a. Input critical temperatures and pressures for all components.
   b. Calculate equation constants a and b.
   c. Compute a and b for vapor mixture.
   d. Compute a and b for liquid mixture.

   Compute Z form of Redlich-Kwong equation of state.
   a. Compute A and B.
   b. Determine roots for the Z form of EOS.
   c. Assign the largest root to the vapor phase root, Z_v.
   d. Assign the smallest root to the liquid phase root, Z_L.

3. Calculate liquid and vapor molar enthalpy in each stage, n
   a. Convert temperature from unit degree Celcius to unit of Kelvin

      t (n) = T_new + 273.15
   b. Calculate ideal molar enthalpy

   c. Calculate liquid molar enthalpy, h_L

      $h_L = \Sigma (y_i h^0_{iv}) + RT [Z_L - 1 - 3A/2B \ln (B/Z_L)]$
   d. Calculate vapor molar enthalpy, h_v

      $h_v = \Sigma (y_i h^0_{iv}) + RT [Z_v - 1 - 3A/2B \ln (B/Z_v)]$

4. Repeat Step 6 to calculate feed, distillate and bottom enthalpy.
5. Calculate condenser and reboiler heat duties
6. Calculate coefficient of energy balance for each stage, j
7. Calculate new vapor flow rates, VE for each tray, j
8. Calculate new liquid flow rates, LE at each tray, j
9. Calculate approximate error of vapor flow rate at each tray j, delV1(j)   and that of liquid flow rate at ach tray j, delL1 (j)
10. Substitute the new values of vapor and liquid flow rates at the component mass balances of Part I of the pseudo code until the approximate errors, delV and delL, are within 0.001.

APPENDIX B: MATLAB PROGRAM CODES

```
%Title: Model of Plate-to-Plate Non-Ideal Mass and Energy Balances of MLNG Depropanizer Column
%Author: Chai Ai Ling
%      (Phase I is modification of Shri Gugan Siva Subramaniam's and Tan Khang Meei's work)
%      Universiti Teknologi Petronas
%      Bandar Seri Iskandar
%      Perak
%Date   20 October 2004
%Assumptions: 1. 100% tray efficiency
%             2. Narrow-boiling feed mixture
%-----------------------------------------------------------------------------------------
% PHASE I
% MASS BALANCE

% Feed parameters
%Ft = input( 'Enter feed rate (tons/day) : ');
%za = input( 'Enter propane fraction in feed : ');
%zb = input( 'Enter isobutane fraction in feed : ');
%zc = input( 'Enter n-butane fraction in feed : ');
%zd = input( 'Enter isopentane fraction in feed : ');
%ze = input( 'Enter n-pentane fraction in feed : ');
%zf = input( 'Enter n-hexane fraction in feed : ');
%q  = input( 'Enter feed quality : ');

% Operational parameters
%xad = input( 'Enter estimated C3 fraction in distillate : ');
%Tf  = input( 'Enter feed temperature (degC) : ');
%RR  = input( 'Enter reflux ratio : ');
%Dt  = input( 'Enter distillate flow rate (tons/day) : ');
%T_con = input( 'Enter condenser operating temperature (degC): ');
%T_reb = input( 'Enter reboiler operating temperature (degC): ');
%P_con = input( 'Enter condenser operating pressure (bar) : ');
%P_feed = input( 'Enter feed operating pressure (bar) : ');

% Geometric parameters
%N  = input( 'Enter number of stages : ');
%Nf = input( 'Enter feed stage number : ');

z = [za zb zc zd ze zf];
nn = [1:N];

% Conversion of user input in from tons/day to mols/hr
F = (Ft * 1000000) / (24 * 58);
D = (Dt * 1000000) / (24 * 58);

%Calculate bottom flow rate, B
B = F-D;
%Liquid flow in rectifying sectio, Lr
Lr = RR*D;
%Liquid flow at stripping section, Ls
Ls = Lr + q*F;
%Liquid flow at each stage for stripping section, L(j)
L(1) = B;
for j = 2 : Nf
    L(j) = Ls;
end
%Liquid flow at each stage on rectifying section, L(k)
for k = (Nf+1):N
    L(k) = Lr;
end

%Vapor flow rate at rectifying section, Vr
Vr = Lr + D;

%Vapor flow in stripping section, Vs
Vs = Vr - (1-q)*F;

%Vapor flow at each stage of stripping section, V(j)
for j = 1:(Nf-1)
    V(j) = Vs;
end
```

59

```
%Vapor flow at each stage for rectifying section, V(k)
for k = Nf:(N-1)
    V(k) = Vr;
end
V(N) = 0;

%Distillate component composition, xid
%Assume equal distribution of isomers in distillate and bottoms
xbd = (zb/(zc+zb))*(1-xad);
xcd = (zc / (zc + zb)) * (1 - xad);
xdd = 0;
xed = 0;
xfd = 0;
xd = [xad xbd xcd xdd xed xfd];

%Bottom component composition, xib
xab = (F*za-D*xad)/B;
xdb = F * zd / B;
xeb = F * ze / B;
xfb = F * zf / B;
xbb = (zb/(zc + zb)) * (1 - xab - xeb - xdb - xfb);
xcb = (zc/(zc + zb)) * (1 - xab - xeb - xdb - xfb);
xb = [xab xbb xcb xdb xeb xfb];

%Temperature at each stage using linear variation from reboiler to condenser
for j = 1 : N;
    T(j) = T_reb + ( (j - 1) / (N - 1) ) * (T_con - T_reb);
end

%Pressure at each stage using linear variation
for j = 1:N;
    P(j) = P_feed + ((j - Nf) / (N-Nf)) * (P_con - P_feed);
end
%K value for each component at each stage
for j = 1 : N
    t = T(j);
    p = P(j);
    ka(j) = fka(t, p);
    kb(j) = fkb(t, p);
    kc(j) = fkc(t, p);
    kd(j) = fkd(t, p);
    ke(j) = fke(t, p);
    kf(j) = fkf(t, p);
end

  K = [ka' kb' kc' kd' ke' kf'];


% Energy balance convergence loop

  counter0 = 0;
  counter1 = 0;
  counter2 = 0;
  for cc = 1:8
      counter0 = counter0 + 1
      for iiii = 1 : 50
          counter1 = counter1 + 1
%theta convergence loop
  counter = 0;
  theta = 1;
  del_theta =1;
  while abs(del_theta) > 1e-3;
% Component mass balance
% Calculate values of elements for matrix ABC, and D
      for j = 1:1;
          Ba(j) = 1 + (V(j) * ka(j)) / B;
          Ca(j) = -1;
          Da(j) = 0;
          Bb(j) = 1 + (V(j) * kb(j)) / B;
          Cb(j) = -1;
          Db(j) = 0;
          Bc(j) = 1 + (V(j) * kc(j)) / B;
          Cc(j) = -1;
```

60

```
    Dc(j) = 0;
    Bd(j) = 1 + (V(j) * kd(j)) / B;
    Cd(j) = -1;
    Dd(j) = 0;
    Be(j) = 1 + (V(j) * ke(j)) / B;
    Ce(j) = -1;
    De(j) = 0;
    Bf(j) = 1 + (V(j) * kf(j)) / B;
    Cf(j) = -1;
    Df(j) = 0;
End

for j = 2 : (Nf-1);
    Aa(j) = -((ka(j-1) * V(j-1)) / L(j-1));
    Ba(j) = 1 + (V(j) * ka(j)) / L(j);
    Ca(j) = -1;
    Da(j) = 0;
    Ab(j) = -((kb(j-1) * V(j-1)) / L(j-1));
    Bb(j) = 1 + (V(j) * kb(j)) / L(j);
    Cb(j) = -1;
    Db(j) = 0;
    Ac(j) = -((kc(j-1) * V(j-1)) / L(j-1));
    Bc(j) = 1 + (V(j) * kc(j)) / L(j);
    Cc(j) = -1;
    Dc(j) = 0;
    Ad(j) = -((kd(j-1) * V(j-1)) / L(j-1));
    Bd(j) = 1 + (V(j) * kd(j)) / L(j);
    Cd(j) = -1;
    Dd(j) = 0;
    Ae(j) = -((ke(j-1) * V(j-1)) / L(j-1));
    Be(j) = 1 + (V(j) * ke(j)) / L(j);
    Ce(j) = -1;
    De(j) = 0;
    Af(j) = -((kf(j-1) * V(j-1)) / L(j-1));
    Bf(j) = 1 + (V(j) * kf(j)) / L(j);
    Cf(j) = -1;
    Df(j) = 0;
end

for j = Nf:Nf;
    Aa(j) = -((ka(j-1) * V(j-1)) / L(j-1));
    Ba(j) = 1 + (V(j) * ka(j)) / L(j);
    Ca(j) = -1;
    Da(j) = F * za;
    Ab(j) = -((kb(j-1) * V(j-1)) / L(j-1));
    Bb(j) = 1 + (V(j) * kb(j)) / L(j);
    Cb(j) = -1;
    Db(j) = F * zb;
    Ac(j) = -((kc(j-1) * V(j-1)) / L(j-1));
    Bc(j) = 1 + (V(j) * kc(j)) / L(j);
    Cc(j) = -1;
    Dc(j) = F * zc;
    Ad(j) = -((kd(j-1) * V(j-1)) / L(j-1));
    Bd(j) = 1 + (V(j) * kd(j)) / L(j);
    Cd(j) = -1;
    Dd(j) = F * zd;
    Ae(j) = -((ke(j-1) * V(j-1)) / L(j-1));
    Be(j) = 1 + (V(j) * ke(j)) / L(j);
    Ce(j) = -1;
    De(j) = F * ze;
    Af(j) = -((kf(j-1) * V(j-1)) / L(j-1));
    Bf(j) = 1 + (V(j) * kf(j)) / L(j);
    Cf(j) = -1;
    Df(j) = F * zf;
end

for j = (Nf+1) : (N-1);
    Aa(j) = -((ka(j-1) * V(j-1)) / L(j-1));
    Ba(j) = 1 + (V(j) * ka(j)) / L(j);
    Ca(j) = -1;
    Da(j) = 0;
    Ab(j) = -((kb(j-1) * V(j-1)) / L(j-1));
```

61

```
    Bb(j) = 1 + (V(j) * kb(j)) / L(j);
    Cb(j) = -1;
    Db(j) = 0;
    Ac(j) = -((kc(j-1) * V(j-1)) / L(j-1));
    Bc(j) = 1 + (V(j) * kc(j)) / L(j);
    Cc(j) = -1;
    Dc(j) = 0;
    Ad(j) = -((kd(j-1) * V(j-1)) / L(j-1));
    Bd(j) = 1 + (V(j) * kd(j)) / L(j);
    Cd(j) = -1;
    Dd(j) = 0;
    Ae(j) = -((ke(j-1) * V(j-1)) / L(j-1));
    Be(j) = 1 + (V(j) * ke(j)) / L(j);
    Ce(j) = -1;
    De(j) = 0;
    Af(j) = -((kf(j-1) * V(j-1)) / L(j-1));
    Bf(j) = 1 + (V(j) * kf(j)) / L(j);
    Cf(j) = -1;
    Df(j) = 0;
end


for j = N:N;
    Aa(j) = -((ka(j-1) * V(j-1)) / L(j-1));
    Ba(j) = 1 + (D / L(j));
    Da(j) = 0;
    Ab(j) = -((kb(j-1) * V(j-1)) / L(j-1));
    Bb(j) = 1 + (D / L(j));
    Db(j) = 0;
    Ac(j) = -((kc(j-1) * V(j-1)) / L(j-1));
    Bc(j) = 1 + (D / L(j));
    Dc(j) = 0;
    Ad(j) = -((kd(j-1) * V(j-1)) / L(j-1));
    Bd(j) = 1 + (D / L(j));
    Dd(j) = 0;
    Ae(j) = -((ke(j-1) * V(j-1)) / L(j-1));
    Be(j) = 1 + (D / L(j));
    De(j) = 0;
    Af(j) = -((kf(j-1) * V(j-1)) / L(j-1));
    Bf(j) = 1 + (D / L(j));
    Df(j) = 0;
end

% Build ABC matrix and set all elements equals to zero

    ABCa = zeros(N);
    ABCb = zeros(N);
    ABCc = zeros(N);
    ABCd = zeros(N);
    ABCe = zeros(N);
    ABCf = zeros(N);

% Insert values for ABC matrix
    for j = 1;
        ABCa(j,j) = Ba(j);
        ABCa(j,(j+1)) = Ca(j);
        ABCb(j,j) = Bb(j);
        ABCb(j,(j+1)) = Cb(j);
        ABCc(j,j) = Bc(j);
        ABCc(j,(j+1)) = Cc(j);
        ABCd(j,j) = Bd(j);
        ABCd(j,(j+1)) = Cd(j);
        ABCe(j,j) = Be(j);
        ABCe(j,(j+1)) = Ce(j);
        ABCf(j,j) = Bf(j);
        ABCf(j,(j+1)) = Cf(j);
    end

    for j = 2 : (N-1);
        ABCa(j,j-1) = Aa(j);
        ABCa(j,j) = Ba(j);
        ABCa(j,(j+1)) = Ca(j);
        ABCb(j,j-1) = Ab(j);
```

62

```
   ABCb(j,j) = Bb(j);
   ABCb(j,(j+1)) = Cb(j);
   ABCc(j,j-1) = Ac(j);
   ABCc(j,j) = Bc(j);
   ABCc(j,(j+1)) = Cc(j);
   ABCd(j,j-1) = Ad(j);
   ABCd(j,j) = Bd(j);
   ABCd(j,(j+1)) = Cd(j);
   ABCe(j,j-1) = Ae(j);
   ABCe(j,j) = Be(j);
   ABCe(j,(j+1)) = Ce(j);
   ABCf(j,j-1) = Af(j);
   ABCf(j,j) = Bf(j);
   ABCf(j,(j+1)) = Cf(j);
end

for j = N;
   ABCa(j,j-1) = Aa(j);
   ABCa(j,j) = Ba(j);
   ABCb(j,j-1) = Ab(j);
   ABCb(j,j) = Bb(j);
   ABCc(j,j-1) = Ac(j);
   ABCc(j,j) = Bc(j);
   ABCd(j,j-1) = Ad(j);
   ABCd(j,j) = Bd(j);
   ABCe(j,j-1) = Ae(j);
   ABCe(j,j) = Be(j);
   ABCf(j,j-1) = Af(j);
   ABCf(j,j) = Bf(j);
end

% Matrix D has also been build automatically
% Solve for component flow rates in matrix I, Ii
% Given that ABC * I = D
   Ia = inv(ABCa) * Da';
   Ib = inv(ABCb) * Db';
   Ic = inv(ABCc) * Dc';
   Id = inv(ABCd) * Dd';
   Ie = inv(ABCe) * De';
   If = inv(ABCf) * Df';
   I = [Ia Ib Ic Id Ie If];

% THETA CONVERGENCE METHOD

% The value of theta is calculated using Newton Raphson method
% fcn1 and fcn2 are function files and are the numerator and denominator of the Newton Raphson

% Input for fcn1 and fcn 2 is taken from the component mass balance
   Iin1 = [I(1,1) I(1,2) I(1,3) I(1,4) I(1,5) I(1,6)];
   Iin2 = [I(N,1) I(N,2) I(N,3) I(N,4) I(N,5) I(N,6)];

% The theta convergence loop is performed to calculate value for theta

ftheta = 1;
   while abs(ftheta) > 1e-3;
      counter = counter + 1
      theta = theta + fcn1(theta, Iin1, Iin2, RR, F,z,D) / fcn2(theta, Iin1, Iin2, RR,F,z)
      if theta < -100
         theta = 1;
      end
      ftheta = fcn1(theta, Iin1, Iin2, RR, F,z,D);
   end

% keep track of number of loops required to find convergence
   counter2 = counter2 + 1

% determine value for testing while loop
   del_theta = abs(1 - theta);

% keep track of number of loops required to find convergence
   counter2 = counter2 + 1
```

```
% Calculate corrected component mole flow rates
% The sum of component flow rates at top, SumD, and bottom, SumB of column should match
% overall mass balance values

 SumD = 0;
 SumB = 0;

 for c = 1 : 6;
    Bxibot_calc(c) = l(1,c);
    Dxidist_calc(c) = l(N,c) / RR;

% The top and bottom component flow rates are corrected using the value of theta
    Dxidist_cor(c) = (F * z(c)) ./ (1 + theta * (Bxibot_calc(c) ./ Dxidist_calc(c)));
    Bxibot_cor(c) = Dxidist_cor(c) * theta * (Bxibot_calc(c) ./ Dxidist_calc(c));
    SumD = SumD + Dxidist_cor(c);
    SumB = SumB + Bxibot_cor(c);
    rm = Dxidist_cor ./ Dxidist_calc;
    sm = Bxibot_cor ./ Bxibot_calc;
 end

 for c = 1 : 6;
    for n = (Nf+1) : N;
       l_cor(n,c) = rm(c) * l(n,c);
    end
    for n = 1 : Nf;
       l_cor(n,c) = sm(c) * l(n,c);
    end
 end

 for n = 1 : N;
    sum_l_cor(n) = 0;
    for c = 1 : 6;
       sum_l_cor(n) = sum_l_cor(n) + l_cor(n,c);
    end
 end

% The component flow rates in the rectifying section are corrected using the ratio of
% corrected to uncorrected top component flow
% The component flow rates in the stripping section are corrected using the ratio of
% corrected to uncorrected bottoms component flow
% Calculate corrected mole fractions for all components at each stage

 for n = 1 : N;
    sumx(n) = 0;
    for c = 1 : 6;
       x(n,c) = l_cor(n,c) / sum_l_cor(n);
       sumx(n) = sumx(n) + x(n,c);
    end
 end

% Calculate new temperatures for each stage
% Bubble point calculation is performed using trial and error until temperature value converges
% fcnT is a function file that is the reverse of function file fka

 for j = 1 : N;
    Kj = [ka(j) kb(j) kc(j) kd(j) ke(j) kf(j)];
    delK = 1.0;
    while abs(delK) > 1e-5;

       for c = 1 : 6;
          Kixi(c) = Kj(c) .* x(j,c);
       end
       ka_new(j) = ka(j) / sum(Kixi);
       ka_fcninput = ka_new(j);
       p = P(j);
       T_new(j) = fcnT(ka_fcninput,p);
       t = T_new(j);
       kb(j) = fkb(t, p);
       kc(j) = fkc(t, p);
       kd(j) = fkd(t, p);
       ke(j) = fke(t, p);
       kf(j) = fkf(t, p);
```

64

```matlab
        Kj = [ka_new(j) kb(j) kc(j) kd(j) ke(j) kf(j)];

        for c = 1 : 6;
            K_new(j,c) = Kj(c);
        end
        delK = ka_new(j) - ka(j);
        ka(j) = ka_new(j);
    end
  end

y = K_new .* x;

end

% End of Constant molar calculation, exit inner loop
% 1 = propane
% 2 = isobutane
% 3 = n-butane
% 4 = isopentane
% 5 = n-pentane
% 6 = n-hexane

for n = 1 : N
    x1(n) = x(n,1);
    x2(n) = x(n,2);
    x3(n) = x(n,3);
    x4(n) = x(n,4);
    x5(n) = x(n,5);
    x6(n) = x(n,6);
    y1(n) = y(n,1);
    y2(n) = y(n,2);
    y3(n) = y(n,3);
    y4(n) = y(n,4);
    y5(n) = y(n,5);
    y6(n) = y(n,6);
end

for j = 1:N
    L_old(j) = L(j);
    V_old (j) = V(j);
end

% Solving Redlich-kwong equation of state

% Input critical constants of components
% 1 = propane
% 2 = isobutane
% 3 = n-butane
% 4 = isopentane
% 5 = n-pentane
% 6 = n-hexane

%Critical temperature, Tc in kelvin(k)
Tc = [369.8  408.2  425.2  460.4  469.7  553.5];

%Critical pressure, Pc in bar
Pc = [4250  3650  3800  3390  3370  4070];

%Calculating equation constants a and b for vapor phase
for n = 1:N
    t(n) = T_new(n);
    T_kel(n) = t(n) + 273.15;
    P_kPa(n) = P(n) * 1e2;
    R = 8.3144e-3;
end

for n = 1:N
    for c = 1:6;
        a(n,c) = (0.42748 * R^2 * Tc(c)^2.5) / (Pc(c) * T_kel(n)^0.5);
        b(n,c) = (0.08664 * R * Tc(c)) / Pc(c);
    end
end
```

65

```
%Calculating mixture constants, a and b
for n = 1:N
   for c = 1:6;
      xi(n,c) = x(n,c);
      yi(n,c) = y(n,c);
   end
end
for n = 1:N
   av_mixture(n) = 0;
   for i = 1:c;
      for j = 1:c;
      av_mixture(n) = av_mixture(n) + ( yi(n,i) .* yi(n,j) .* (a(n,i) .* a(n,j))^0.5);
      end
   end
end

for n = 1:N
   bv_mixture(n) = 0;
   for i = 1:c;
      bv_mixture(n) = bv_mixture(n) + ( yi(n,i) .* b(n,i) );
   end
end
%Calculating compressibility factor, Z of R-k equation

%Calculate A and B
for n = 1:N;
   Av(n) = (av_mixture(n) * P_kPa(n)) / ( R^2 * T_kel(n)^2 );
   Bv(n) = (bv_mixture(n) * P_kPa(n)) / (R * T_kel(n));
end

%Solve for roots of Z form of R-K equation
%fZ = Z3 - Z2 + (A - B - B2)Z - AB
% Zv(n) = max(roots(fZv))       Largest root = Vapor phase
% Zl(n) = min(roots(fZl))       Smallest root = Liquid phase

for n = 1:N
   fZv = [1 -1 (Av(n) - Bv(n) - Bv(n)^2) -Av(n)*Bv(n)];
   Zv(n) = max(roots(fZv));
end

for n = 1:N;
   al_mixture(n) = 0;
   for i = 1:c;
      for j = 1:c;
      al_mixture(n) = al_mixture(n) + ( xi(n,i) * xi(n,j) * (a(n,i) * a(n,j))^0.5 );
      end
   end

end

for n = 1:N
   bl_mixture(n) = 0;
   for i = 1:c;
      bl_mixture(n) = bl_mixture(n) + ( xi(n,i) .* b(n,i) );
   end

end

%Calculating compressibility factor, Z of R-k equation

for n = 1:N
   Al(n) = (al_mixture(n) * P_kPa(n)) / (R^2 * T_kel(n)^2);
   Bl(n) = (bl_mixture(n) * P_kPa(n)) / (R * T_kel(n));
end
for n = 1:N
   fZl = [1 -1 (Al(n) - Bl(n) - Bl(n)^2) -Al(n)*Bl(n)];
   Zl(n) = min(roots(fZl));
end

% ENTHALPY BALANCE
```

66

```matlab
% Molar enthalpy for vapor and liquid in each stage
% Vapor phase
for n = 1:N
    R = 8.314e-3;        %Gas constant (kJ/mol.K)
    for c = 1:6;
        xi(n,c) = x(n,c);
        yi(n,c) = y(n,c);
        %Constant for Heat Capacity Cp
        a_Cp = [1.212768 1.67674 2.240853 2.423523 2.974049 3.762599];
        b_Cp = [0.028782 0.037849 0.036368 0.046088 0.04451 0.052548];
        c_Cp = [-0.0000088 -0.000012 -0.000011 -0.000015 -0.000014 -0.000016];
        d_Cp = [0 0 0 0 0 0];

        %Calculate hvo
        hvo(n,c) = (a_Cp(c) * R * T_kel(n)) + (b_Cp(c)*R*T_kel(n)^2 / 2) + (c_Cp(c) * R*T_kel(n)^3 / 3);
        %Constants for Hvap
        c1 = [2.9209e7 3.1667e7 3.6238e7 3.77e7 3.9109e7 4.4544e7];
        c2 = [0.78237 0.3855 0.8337 0.3952 0.38681 0.39002];
        c3 = [-0.77319 0 -0.82274 0 0 0];
        c4 = [0.39246 0 0.39613 0 0 0];
        Tc = [369.83 408.14 425.12 460.43 469.7 507.6];

        Tr(n,c) = T_kel(n) / Tc(c);
        hvap(n,c) = c1(c)*((1-Tr(n,c))^(c2(c)+(c3(c)*Tr(n,c))+(c4(c)*(Tr(n,c)^2))));     % Calculate Hvap
        Hvap(n,c) = 1e-6 * hvap(n,c);       %convert hvap from J/kmol to kJ/mol

        if T_kel(n) > 369.83
            Hvap (n,1) = 0;
        end
        if T_kel(n) > 408.14
            Hvap(n,2) = 0;
        end
        if T_kel(n) > 425.12
            Hvap (n,3) = 0;
        end
        if T_kel(n) > 460.43
            Hvap(n,4) = 0;
        end
        if T_kel(n) > 469.7
            Hvap (n,5) = 0;
        end
        if T_kel(n) > 507.6
            Hvap(n,6) = 0;
        end

        H(n,c) = yi(n,c) * hvo(n,c);
        h(n,c) = xi(n,c) * (hvo(n,c) - Hvap(n,c));
    end

% Account for non-ideality in mxiture
    H_sum(n) = H(n,1) + H(n,2) + H(n,3) + H(n,4) + H(n,5) + H(n,6);    %Vapor molar enthalpy
    h_sum(n) = h(n,1) + h(n,2) + h(n,3) + h(n,4) + h(n,5) + h(n,6);    %Liquid molar enthalpy

    H(n) = H_sum(n) + R * T_kel(n) * (Zv(n) - 1 - 3*Av(n)/2*Bv(n)*log(Bv(n)/Zv(n)) );
    h(n) = h_sum(n) + R * T_kel(n) * (Zl(n) - 1 - 3*Al(n)/2*Bl(n)*log(Bl(n)/Zl(n)) );
end

% Calculate distillate enthalpy

td = T_kel(N);
R = 8.314e-3;
xind = xd;

for c = 1:6
    %Constant for Heat Capacity Cp
    ad = [1.212768 1.67674 2.240853 2.423523 2.974049 3.762599];
    bd = [0.028782 0.037849 0.036368 0.046088 0.04451 0.052548];
    cd_Cp= [-0.0000088 -0.000012 -0.000011 -0.000015 -0.000014 -0.000016];
    dd = [0 0 0 0 0 0];
    %Calulate hvo
    hvod(c) = (ad(c) * R * td) + (bd(c) * R * td^2 / 2) + (cd_Cp(c) * R * td^3 / 3);
    %Calculate distiallate ideal enthalpy
```

67

```
    hDc(c) = xind(c) * hvod(c);
end

hD = sum(hDc) + + R * td * (ZI(N) - 1 - 3*AI(N)/2*BI(N)*log(BI(N)/ZI(N)) );

QN = D * (1 + RR) * (hD - H(N-1));

%calculate feed enthalpy

Tf_kel = T_kel(Nf) + 273.15;
xf = z;
R = 8.314e-3;
    for c = 1:6
        %Constants for Heat capacity Cp
        af = [1.212768 1.67674 2.240853 2.423523 2.974049 3.762599];
        bf = [0.028782 0.037849 0.036368 0.046088 0.04451 0.052548];
        cf_Cp = [-0.0000088 -0.000012 -0.000011 -0.000015 -0.000014 -0.000016];
        df = [0 0 0 0 0 0];
        %Calculate hvo
        hvof(c) = (af(c) * R * Tf_kel) + (bf(c) * R * Tf_kel^2 / 2) + (cf_Cp(c) * R * Tf_kel^3 / 3);
        hFc(c) = xf(c) * hvof(c);
    end
    hF = sum(hFc) + R * Tf_kel * (ZI(Nf) - 1 - 3*AI(Nf)/2*BI(Nf) * log(BI(Nf)/ZI(Nf)));

% Calculate bottom enthalpy

Tre_kel = T_kel(1);
xin_re = xb;
R = 8.314E-3;
    for c = 1:6
        %Constants for Heat capacity Cp
        a_re = [1.212768 1.67674 2.240853 2.423523 2.974049 3.762599];
        b_re = [0.028782 0.037849 0.036368 0.046088 0.04451 0.052548];
        c_re = [-0.0000088 -0.000012 -0.000011 -0.000015 -0.000014 -0.000016];
        d_re = [0 0 0 0 0 0];
        hvo_re(c) = (a_re(c) * R * Tre_kel) + (b_re(c) * R * Tre_kel^2 / 2) + (c_re(c) * R * Tre_kel^3/ 3);

        %Calculate ideal enthalpy
        hc_re(c) = xin_re(c) * hvo_re(c) ;
    end

    hB = sum(hc_re) + R * Tre_kel * (ZI(1) - 1 - 3*AI(1)/2*BI(1) * log(BI(1)/ZI(1)));

Q1 = (D * hD) + (B * hB) - (F * hF) - QN;

AE(1) =0;
BE(1) = H(1)-h(2);
DE(1) = Q1 + B*(h(2)-h(1));
for j = 2 : (Nf-1)
    AE(j) = h(j) - H(j-1);
    BE(j) = H(j) - h(j+1);
    DE(j) = B * (h(j+1) - h(j));
end
AE(Nf) = h(Nf) - H(Nf-1);
BE(Nf) = H(Nf) - h(Nf+1);
DE(Nf) = (F * hF) + B * (h(Nf+1) - h(Nf))- (F * h(Nf+1));
    for j = (Nf+1) : (N-1)
    AE(j) = h(j) - H(j-1);
    BE(j) = H(j) - h(j+1);
    DE(j) = B * (h(j+1) - h(j))+ (F * h(j))- (F * h(j+1));
    end

    VE(1) = DE(1)/BE(1);

    for j = 2:(N-1);
        VE(j) = ( DE(j)- (AE(j)*VE(j-1)) )/BE(j);
    end

    VE(N) = 0;

    LE(1) = B;
    for j = 2:(Nf-1)
```

```
    LE(j) = VE(j-1)+ B;
end

LE(Nf) = VE(Nf-1) + B;

for j = (Nf + 1): (N-1)
    LE(j) = VE(j-1) + B - F;
end

LE(N) = RR * D;

for j = 1:N-1
    delV1(j) = (VE(j) - V_old(j))/VE(j);
    delL1(j) = (LE(j) - L_old(j))/LE(j);
end

delV(cc) =(VE(cc) - V_old(cc))/VE(cc);
delL(cc) = (LE(cc) - L_old(cc))/LE(cc);

    if abs(delV(cc)) < 1e-3
    if abs(delL(cc)) < 1e-3
        Vfinal(cc) = VE(cc);
        Lfinal (cc) = LE(cc);
    else
        Vfinal(cc) = VE(cc);
        L(cc) = LE(cc);
    end
    else
        if abs(delL(cc)) < 1e-3
        V(cc) = VE(cc);
        Lfinal(cc) = LE(cc);
    else
        L(cc) = LE(cc);
        V(cc) = VE(cc)
    end
    end
end

    disp('Vfinal is')
    disp(Vfinal)
    disp('*************************************************************')
    disp('Lfinal is')
    disp(Lfinal)

    plot(nn, x1, nn, x2, nn, x3, nn, x4, nn, x5, nn, x6)
    title('Liquid Composition Profiles')
    xlabel('Tray number')
    ylabel('Liquid mole fraction, x')
    legend('C3', 'i-C4', 'n-C4', 'i-C5', 'n-C5', 'n-C6')
    pause

    plot(nn, Vfinal, nn, Lfinal)
    title('Converged Vapor and Liquid Flow Rate for Each Tray')
    xlabel('Tray number')
    ylabel('Flow rate, mol/hr')
    legend('Vapor','Liquid')
    pause

    plot(nn, y1, nn, y2, nn, y3, nn, y4, nn, y5, nn, y6)
    title('Vapor Composition Profiles')
    xlabel('Tray number')
    ylabel('Vapor mole fraction, y')
    legend('C3', 'i-C4','n-C4', 'i-C5','n-C5','n-C6')
    pause

    plot(nn, T_new, nn, T)
    title('Temperature Profile')
    xlabel('Tray number')
    ylabel('Temperature, oC')
    legend('Converged temperature', 'Initial assumed temperature')
    end
```
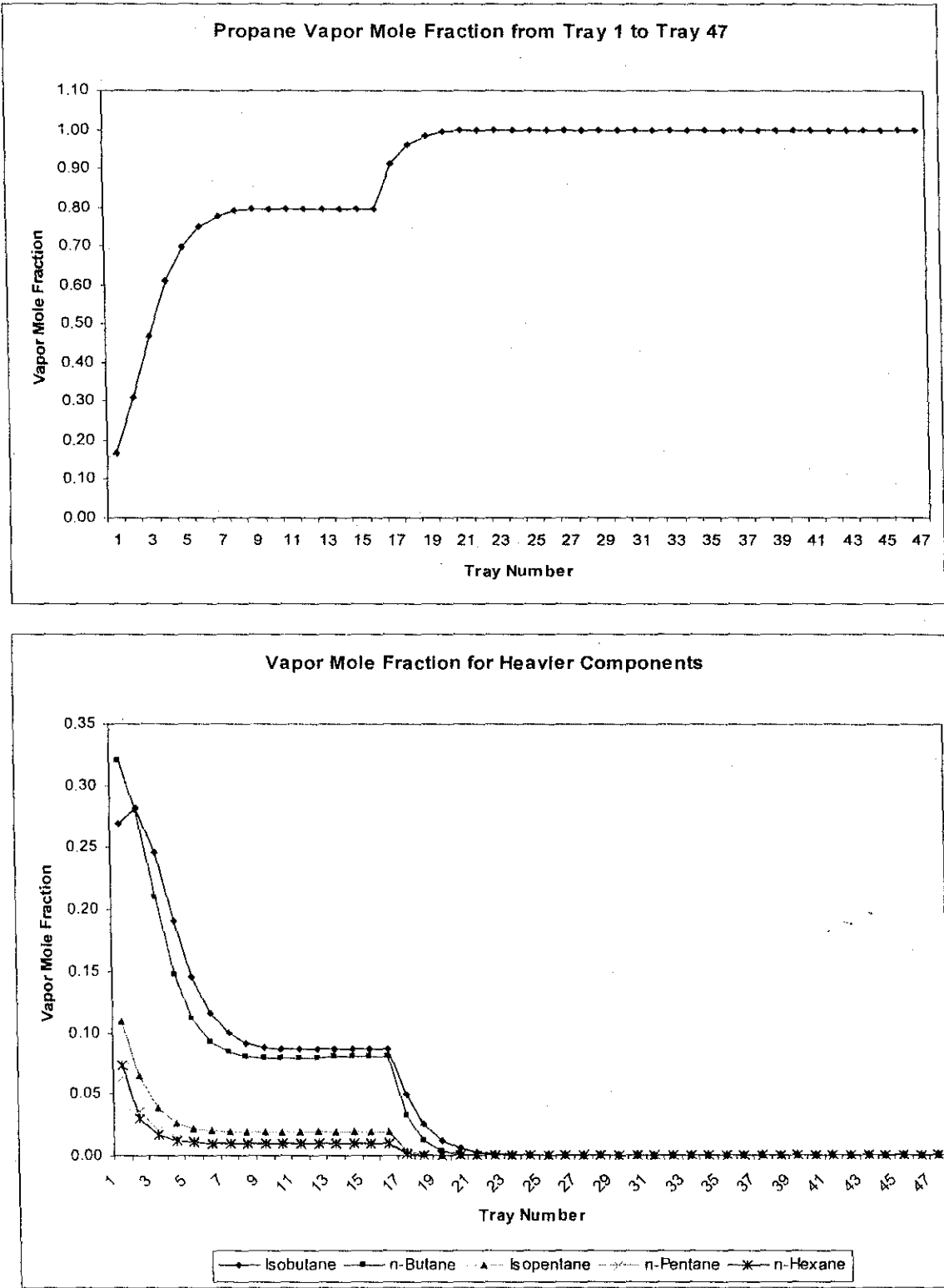
69

APPENDIX C: MODEL RESULTS

Figure C1 Vapor composition of Propane and Heavier Components

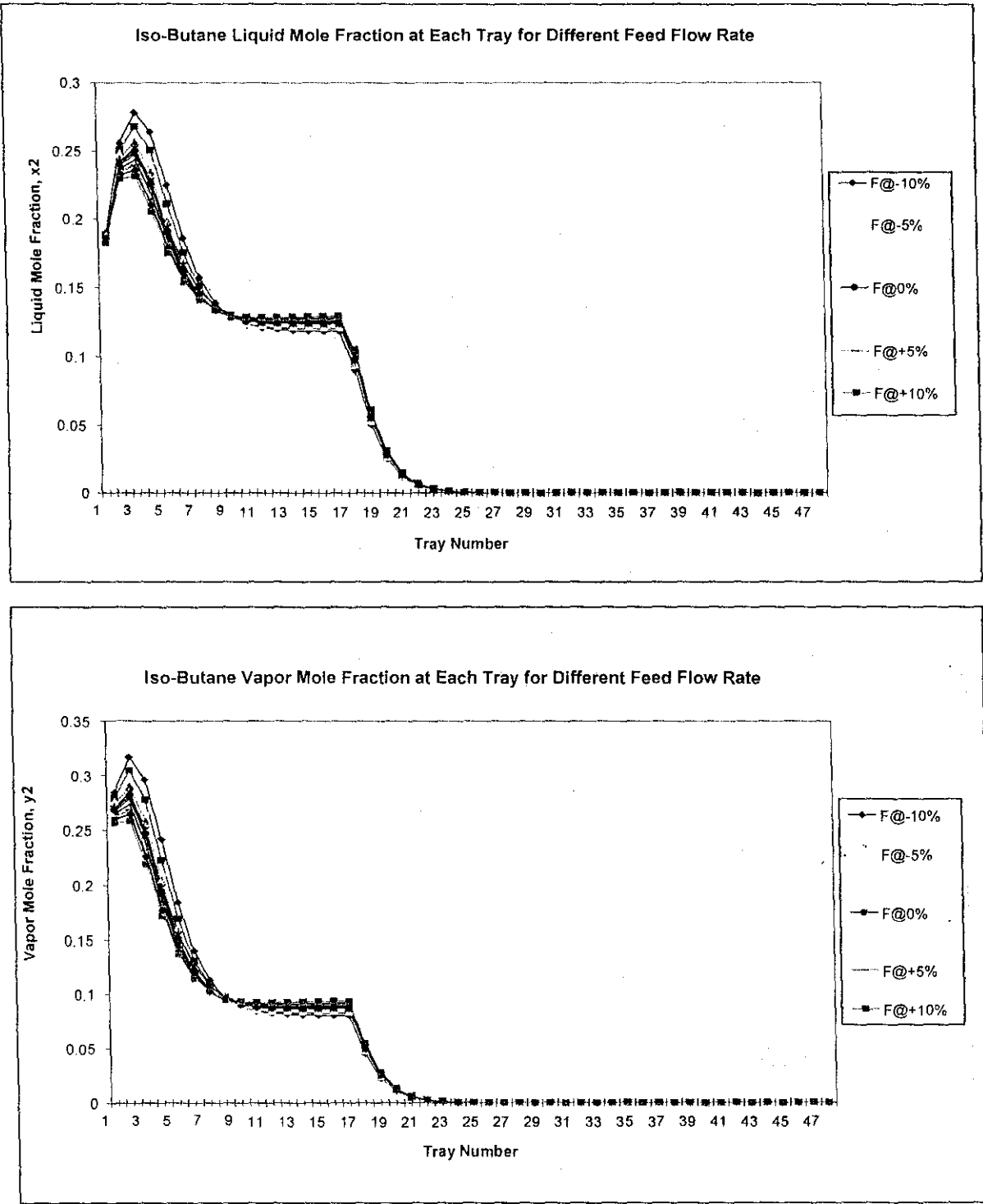# APPENDIX D: "WHAT IF" ANALYSIS RESULTS

Variation of Feed Flow Rate

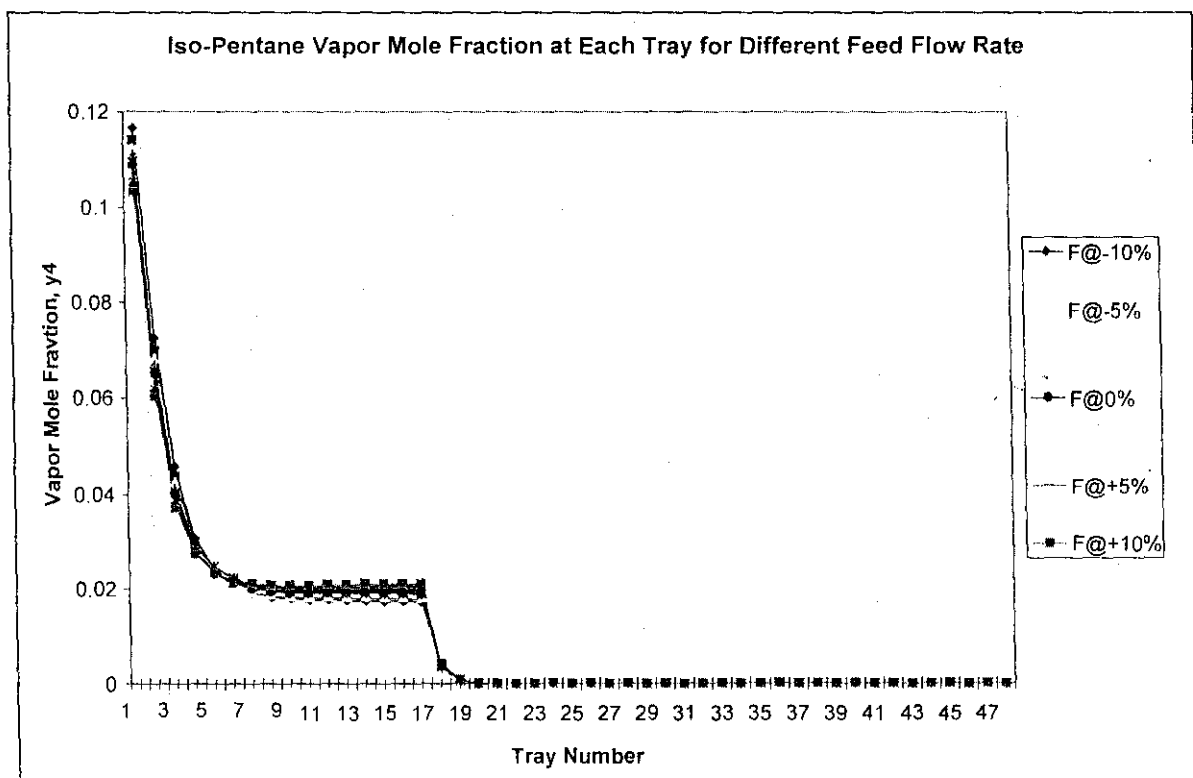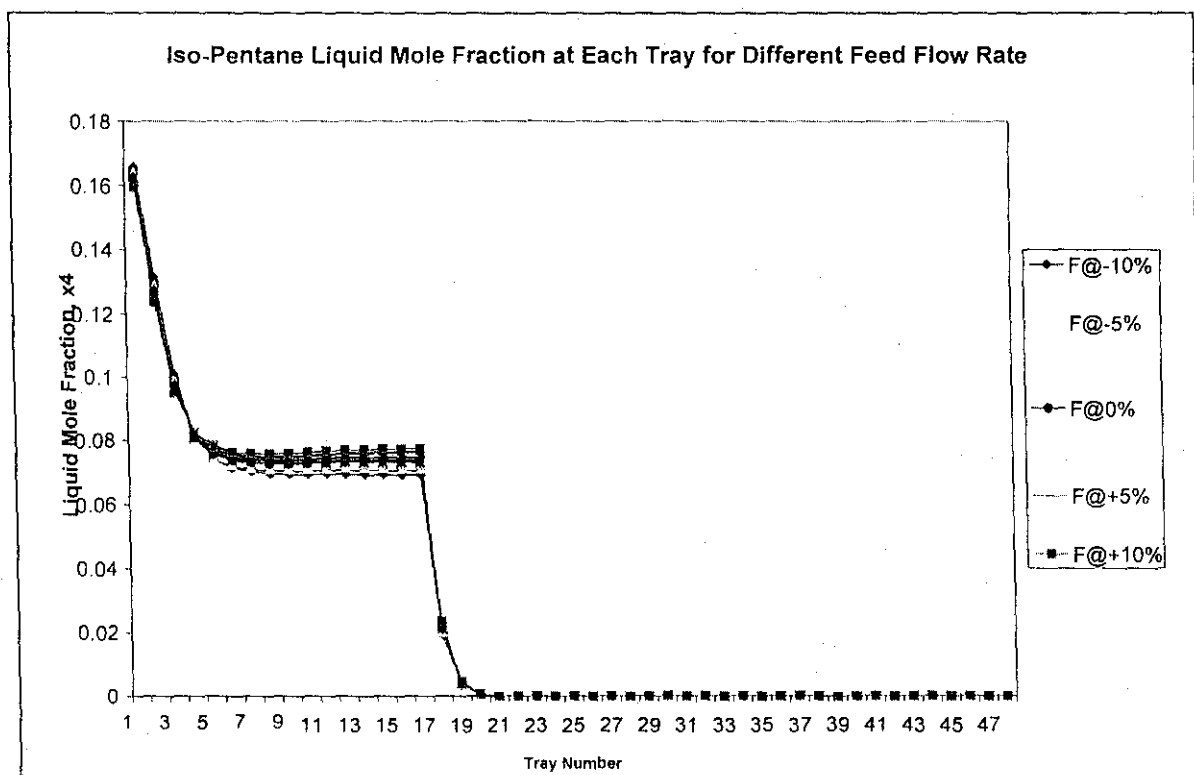Figure D1 Iso-butane composition profile at different feed flow rate

Figure D2 Iso-pentane composition profile at different feed flow rate
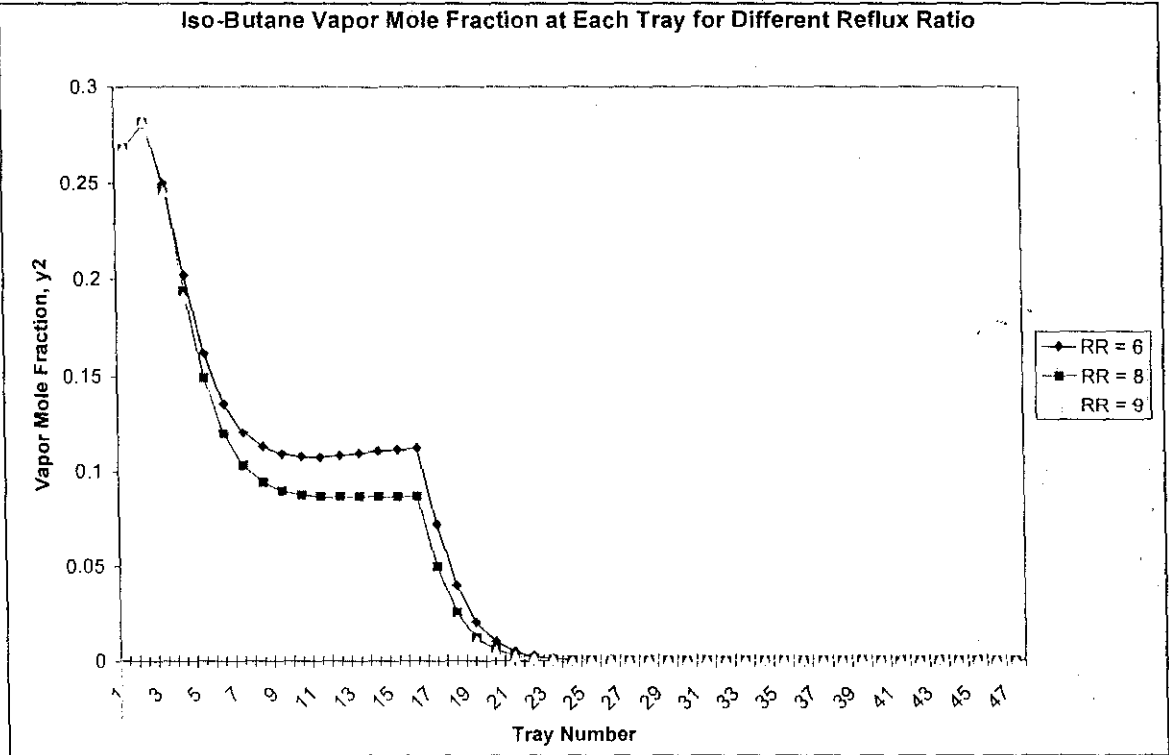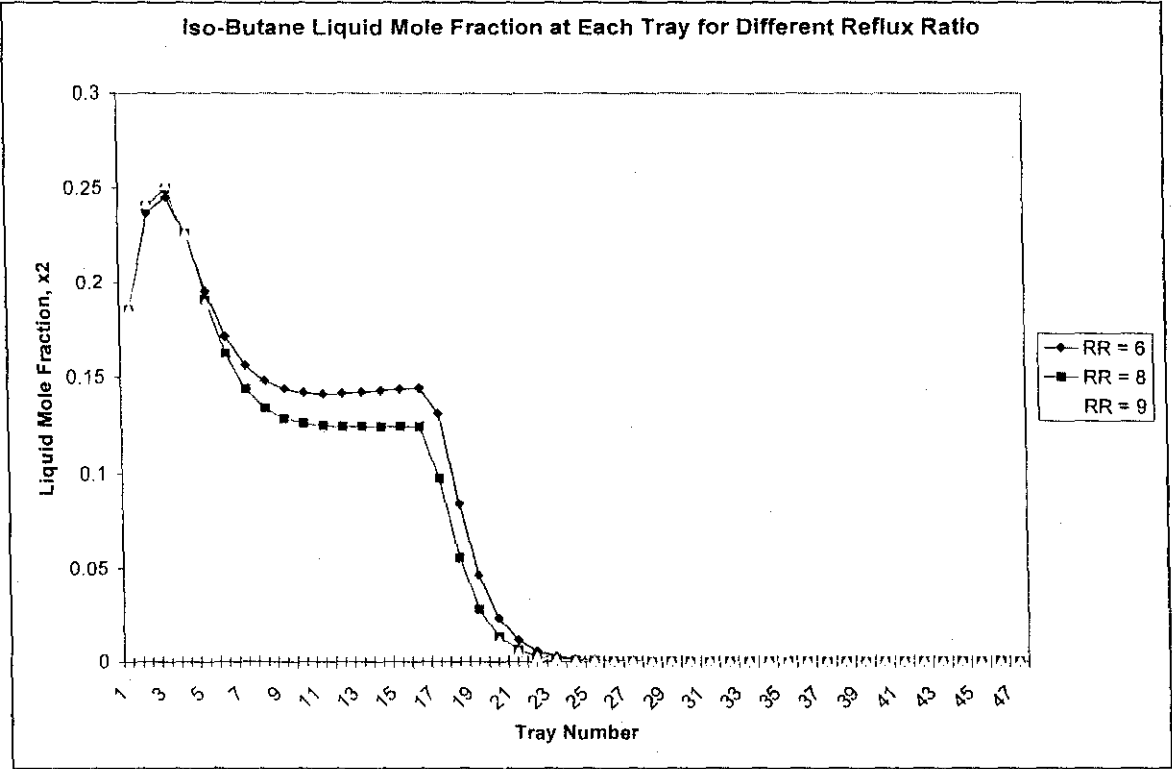
Variation of Reflux Ratio

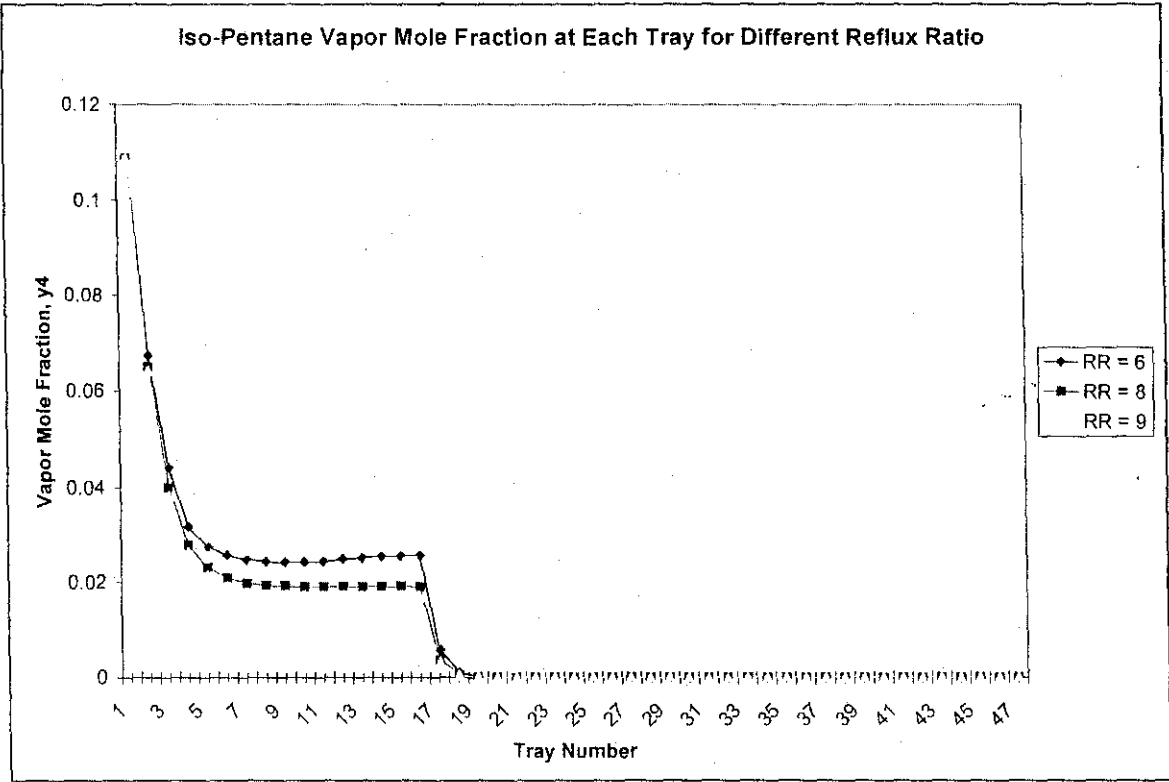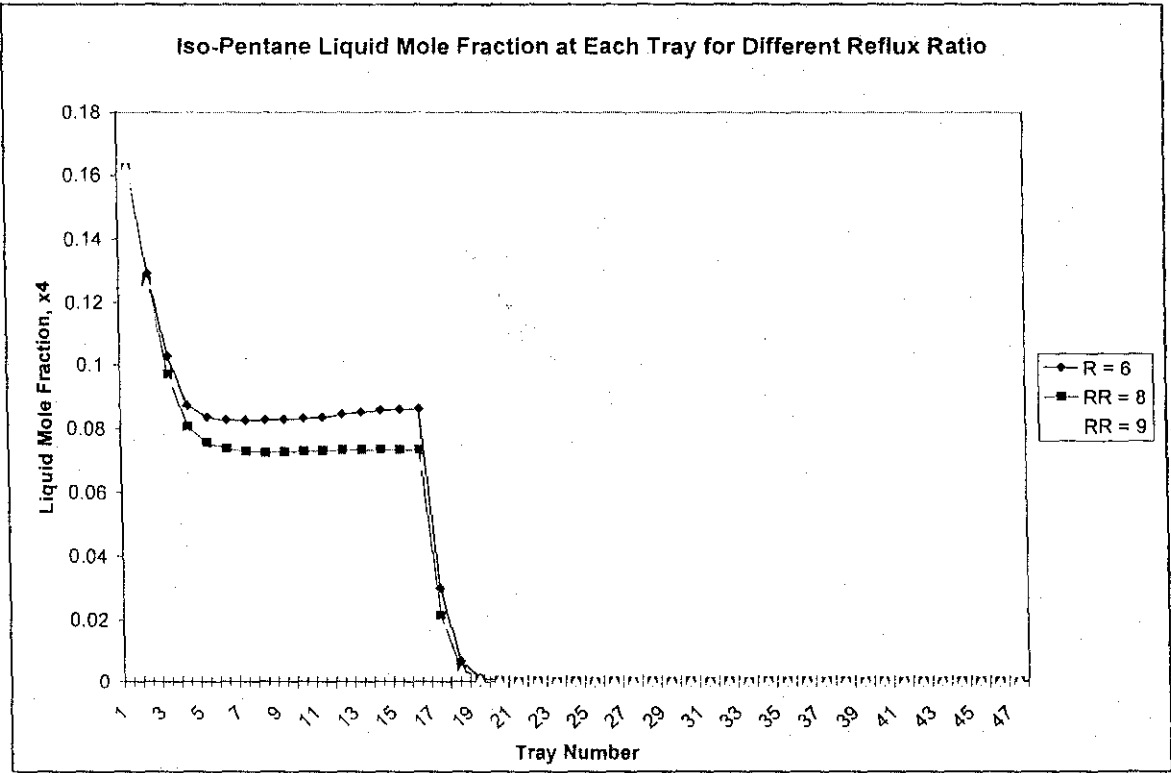Figure D5 Iso-butane composition profile at different reflux ratio

73

Figure D6 Iso-pentane composition profile at different reflux ratio